HIGH-PERFORMANCE MULTIMODAL APPROACH FOR DEFECT IDENTIFICATION IN KNITTED AND WOVEN FABRIC

Pallemullage Sajith Harshana Pallemulla

(188119K)

Degree of Master of Philosophy

Department of Computer Science and Engineering

University of Moratuwa

Sri Lanka

August 2022

HIGH-PERFORMANCE MULTIMODAL APPROACH FOR DEFECT IDENTIFICATION IN KNITTED AND WOVEN FABRIC

Pallemullage Sajith Harshana Pallemulla

(188119K)

Thesis submitted in partial fulfillment of the requirements for the degree Master of Philosophy in Computer Science and Engineering

Department of Computer Science and Engineering

University of Moratuwa

Sri Lanka

August 2022

Declaration

I declare that this is my own thesis and this thesis does not incorporate, without acknowledgement, any material previously submitted for a Degree or Diploma in any other university or institute of higher learning and to the best of my knowledge and belief it does not contain any material previously published or written by another person except where the acknowledgement is made in the text.

Also, I hereby grant to University of Moratuwa the non-exclusive right to reproduce and distribute my thesis, in whole or in part in print, electronic or other medium. I retain the right to use this content in whole or part in future works (such as articles or books).

Signature: Date:

....

PSH Pallemulla

The above candidate has carried out research for the MPhil thesis under my supervision.

Signature of the Supervisor(s): Date:

....

Dr. Chathura de Silva

....

Dr. (Mrs.) Sulochana Sooriyarachchi

Acknowledgements

This research was supported by the Accelerating Higher Education Expansion and Development (AHEAD) Operation of the Ministry of Higher Education funded by the World Bank.

I am extremely grateful to my supervisors, Dr. Chathura R. de Silva and Dr. Sulochana J. Sooriyaarachchi along with the deputy project coordinator of the FabVis project, Prof. Chandana D. Gamage, for their invaluable input and guidance throughout the research.

Abstract

Fabric inspection is a key quality assurance process in the garment industry as it involves the detection of defects in a fabric roll prior to being sent for production. Many studies have been conducted on defect identification in either knitted or woven fabrics, but only a few have considered both types. In this paper, a method for detecting defects in both knitted and woven fabrics is proposed. The method involves extracting co-occurrence, wavelet and local entropy features from a fabric image and classifying the image as defective or defect-free using a classifier with these features given as input. Five commonly-used classifiers were tested. This method was applied to a dataset with seventeen different types of defects and an overall classification accuracy of 93.31% was achieved by the k-nearest neighbours classifier.

Keywords:

fabric inspection, defect detection, co-occurrence, wavelet, local entropy

Table of Contents

List of Figures

List of Tables

Section 1
Introduction

1.1 Background

Quality is an important aspect in the textile industry for competing effectively in the global market. Improved quality is among the major approaches for increasing profitability of the textile industry, along with increased automation, flexibility in production and quick response to customer needs [6]

Fabric inspection is a process that is carried out prior to the fabric being sent out for production into clothing items. In this process, rolls of fabric are fed into a machine that unwinds the roll gradually. The employee carrying out the inspection will observe the fabric being unwound and spot defects in the fabric. Due to this being a tedious process, only about 70% of defects can be detected by even the most highly-trained inspectors [7]. If the defective fabrics that pass inspection are produced into clothing and sold, the company will have to face customer returns and customer claims [8]. Among the defects found in the garment industry, 85% are attributed to fabric defects [9], in contrast with defects during production. Therefore, the accuracy of the fabric inspection process is of vital importance. Nowadays, many segments of the industry are working towards just-in-time delivery and a poor quality production run can be disastrous [10].

Fabric defects are local anomalies in the fabric texture [11]. There are many types of defects that can occur in fabrics. Patel et al. claims that there can be as many as 235 different types [12]. Defects can occur due to a variety of reasons, including inferior yarn quality, improper machine parameters, faulty machine parts and unskilled machine operators [13]. The classification of defects is important

as the type of defect will help find its cause. Once the defect is identified, maintenance personnel will be able to take necessary action to prevent the defect from being reproduced.

Defect detection is classifying a fabric as defective or defect-free and defect classification is the process of identifying the type of the defect. The methods that have been used for defect detection can be broadly categorized into three: statistical, spectral and model-based methods [14] [15]. Although much research has been conducted using these methods, surveys [14] [16] [17] conclude that every method has its limitations. A similar conclusion can be arrived at with defect classification algorithms of which Artificial Neural Networks (ANNs), Support Vector Machines (SVMs), clustering algorithms and statistical inference are the most prominent [18] [19]. Reviews and surveys conducted on fabric defect identification [14] [17] [19] agree that a combination of defect identification techniques will give better results than either one individually.

1.1.1 Research Problem

Research that addresses defect detection in both knitted and woven fabric is scarce. Past studies show that techniques excelling at detecting defects on one type of fabric (knitted or woven) does not always work on the other because the properties of the yarn structure in these fabrics are different from each other [20]. Garment manufacturers who ship to international clients produce apparel from both knit and woven fabrics. Therefore, an algorithm that is capable of detecting defects of both fabric types is preferred for automated inspection.

Owing to the dearth of manual labour and the cost of employment [21], the ultimate goal of industrial automation in the apparel manufacturing industry is minimal human intervention. In fabric inspection, manual labour is used for loading the fabric roll onto the machine, inspecting the fabric and reporting the identified defects. If this process were to be fully-automated, all three of the afore-

mentioned steps must be automated individually. Currently, no algorithm exists for separately identifying knit fabric from woven fabric. This binary classification is not a trivial problem, because some knit material closely resemble woven material when visually observed. Consequently, even if such a classification is implemented in a fully-automated, image-processing-driven defect identification system, its result will not necessarily be the manufacturer's classification of the fabric. So, if two different algorithms are required for defect detection in knit and woven fabric, manual input of the manufacturer's classification will be necessary to select the appropriate algorithm for the loaded fabric type. A single algorithm for defect detection in both types of fabric eliminates the need for such intervention.

1.1.2 Research Objectives

The goal of this research is to develop a method to detect a wide range of defects that occur in both knitted and woven fabrics.

The objectives of this research are

- To select and optimize a set of algorithms to extract features from images of fabric.
- To use the features extracted from said algorithms to classify images of fabric as defective or defect-free.

Defect detection is the term used for separating images of defective fabric from defect-free fabric — a binary classification. A multimodal approach is used so that the strengths of multiple feature extraction algorithms can be combined to achieve an accurate detection. Three algorithms that have shown the capacity of detecting a wide range of defects with high accuracies have been selected, based on the multitude of past studies done in this area. These algorithms, and the preprocessing steps that they follow, are then optimized to extract a set of

features that reliably quantify different characteristics of the fabric.

Subsequently, these features are provided as input to commonly-used classification algorithms in the domain of defect detection. Multiple iterations of training are carried out using cross-validation, thereby tuning the classifiers' hyperparameters in order to achieve the highest possible accuracies for each classifier. Furthermore, a classifier-independent feature ranking based on mutual information is used to identify any features that do not contribute, or contribute negatively to classifier performance.

Even though it is not addressed in this research, it should be noted that "defect classification" is the term used for labelling each defective image with the type of defect present in it.

1.1.3 Research Contributions

This research has two main contributions. First, we propose a novel combination of features to capture the distinguishing characteristics of defective and defect-free fabrics. Second, we show that our method is applicable to a wide range of defects that occur in both knitted and woven fabrics, given that the fabrics are unpatterned and unprinted.

1.2 Outline of Thesis

The rest of the thesis is organized as follows. Section 2 presents a review of similar studies on fabric defect identification including state-of-the-art methods. Section 3 presents an overview of the methodology. Section 4 presents the feature extraction and defect identification processes. Section 5 presents the experimental results and the discussion of said results, followed by conclusions and suggestions for future improvements in the area in Section 6.

Section 2

Literature Review

This chapter presents a review of the literature related to fabric detection and classification. The need for automating fabric inspection is described along with the challenges that come with it. Furthermore, the various techniques for detecting and classifying defects used in past research are discussed.

2.1 Fabric Defects

The absence of a comprehensive dataset of fabric defects has been a major obstacle for many researchers. The Textile-Texture Database (TILDA) database, realized by the Technische Universität Hamburg in 1995 has been used by several research [22] [23] to benchmark their algorithms. It consists of 3200 images of 4 types of fabrics and 7 types of defects. This dataset is the largest fabric defect database in existence. However, due to the small number of defect types represented, the lower quality of the imaging system used and the random orientations of the textiles imaged, this dataset has a limited capacity of being a comprehensive one. Most researchers have used their own datasets for their research and the number of samples included in those datasets are comparatively fewer.

In order to widen the research scope, a total of 17 defect types were selected. They are Abrasion Mark, Broken End, Broken Pick, Burl, Coarse End, Coarse Pick, Colour Fly, Dirty Yarn, Dropped Stitches, Foreign Yarn, Hole, Knot, Missing Yarn, Oil Spot, Slub, Thick Place and Thin Place. These defects include the ones that are most commonly seen in fabric inspection in the industry, as verified by experts. Details of the dataset's creation are in Section 3.2.

2.2 Fabric Inspection

The term "fabric inspection" refers to the process of checking a fabric roll for defects. It is a quality assurance process and is adopted by both fabric manufacturers and garment manufacturers. Fabric manufacturers carry out inspection as the final step in their quality control pipeline, before the fabric rolls are shipped to their clients e.g. garment manufacturers. Garment manufacturers subject fabric rolls to inspection as the first step in their quality control pipeline, before the rolls are sent to the production floor. Since a large number of fabrics are produced and inspection is prevalently carried out by human inspectors in the industry, it is infeasible for a 100% inspection. Therefore, fabric manufacturers and garment manufacturers alike resort to sampling inspection of fabric rolls.

2.2.1 Visual Fabric Inspection

Fabric inspection is largely carried out visually, by a human. The most common method used by many segments in the textile industry is to load the fabric roll onto an inspection machine, let the machine unroll the fabric and have a human inspector observe it for defects. The fabric, which is typically 1.5 — 2 m wide, is usually unrolled at a rate of 8 — 20 m/min [14]. When the inspector notices a defect on the unrolling fabric, he stops the machine, records the type and location of the defect and restarts the machine. If the same type of defect is repetitive or if the rate of the defects are too high, the production department will be alerted so that they can take measures to rectify any errors in production.

Visual inspection is not carried out at the machine that produces the fabric. After a sufficient amount of fabric has been produced, it is removed from the production machine, batched into rolls and then sent to the inspection station [24]. The reasons for inspection not being done simultaneously with production are two-fold — the slow manufacturing speed of the fabric is inadequate to keep a

human inspector occupied and the environment near the production machine is relatively hostile [25].

The time-consuming process of human visual inspection results in some defects going unnoticed. Moreover, defect classification by a human can be subjective due to there being a large number of defects that are characterized by their vagueness and ambiguity [18].

2.2.2 Automated Fabric Inspection

Visual fabric inspection suffers two major drawbacks. They are low speed and poor accuracy.

As fabric inspection is a bottleneck in the apparel manufacturing process, speeding it up would cause the entire process to be faster. However, when a human inspector is tasked with the job, the inspection machine has to be run at slower speeds, because it will be difficult for the human eye to reliably spot defects at higher speeds. In order to utilize the higher speeds that are available in the inspection machine for defect detection, an automated solution is required.

Even when the machine is running at relatively slow speeds (around 8 m/min), it has been found that even expert inspectors miss roughly 70% [7] of the defects. This is due to inspectors getting fatigued and distracted during the long hours they work to meet the day's goals. An automated solution will not have these drawbacks and therefore will be more accurate and reliable in their operation.

Since visual fabric inspection is the norm in most apparel manufacturing plants, it is often impossible to inspect an entire batch of rolls which are slated for use in a particular day. Therefore, only a few rolls are inspected as a sample. The decision to utilize or discard the rest of the rolls in the batch is made from the results of the sample. If a batch is to be discarded, there is an enormous waste of resources, including the time taken for inspection. An automated system of

sufficient speed will be able to carry out inspection of the entire batch or at least more samples. If the system is fast enough to inspect all rolls in a batch with a high accuracy, then it will be able to provide data on exact defect locations. These data can be used by the cutting section to still use a portion of the fabric roll rather than discarding it in its entirety. If the system is not fast enough to inspect all the rolls in a batch, it will still be able to inspect more rolls than a human in the same amount of time, thus increasing the sample size and therefore produce a more precise estimate of the quality of the batch.

Using an automated system also circumvents the cost and time taken for the training of human inspectors. However, it should be noted that most commercially-available systems come with a substantial installation cost and requires regular maintenance.

2.3 Image Processing in Fabric Inspection

The traditional method of fabric inspection is centred around the human visual system. Thus, image processing is the most obvious method of replacing it. Image processing also carries with it several advantages such as the low cost of hardware required for its implementation and its ability to be integrated to an existing inspection machine with minimal modifications.

2.3.1 Challenges

Visual inspection is automated using algorithms in the field of image processing. Based on the many studies conducted on automated fabric defect detection, researchers have faced a number of challenges:

1. The large number of defect types that occur in fabrics is a challenge, especially when considering defect classification. The lack of a database in which most, if not all, of the defect types are represented exacerbates this issue.

2. The inter-class similarity in defects makes it difficult for algorithms to reliably discriminate between some defects. For example, broken picks and broken ends in the same fabric can sometimes be almost indistinguishable. Inspectors distinguish between some slubs and small knots by touch because on occasion, they look similar.

3. The same defect manifests across multiple fabric types in different forms. For example, abrasion marks are caused by frictional damage to the fabric. A cotton fabric and a synthetic fabric respond differently to frictional wear and therefore, abrasion marks on these fabrics do not look alike.

4. The characterization of defects in fabric is generally not well-defined.

5. Images captured during inspection suffer from noise arising from the environment and from hardware. Dust and stray yarn is generated by the constant rolling of fabrics over rollers in an inspection area. These deposit on the surface of the fabric under the image sensor. The image sensor and hardware interfacing will give rise to multiple types of noise in the images.

2.3.2 Defect Detection Methods

Fabric defect detection algorithms attempt to classify fabrics as defective or defect-free. Based on the features extracted from the fabric image, these algorithms are classified into three, namely, spatial, spectral and model-based [14] [15] as shown in Figure 2.1.

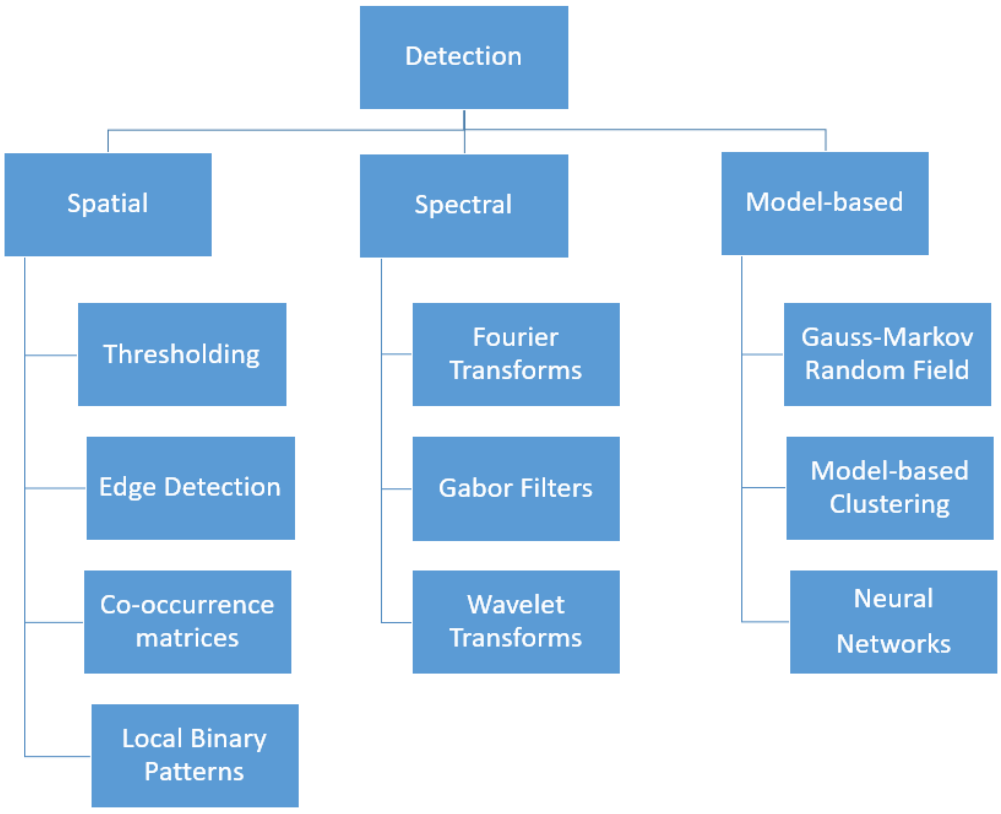

Figure 2.1: Categorization of fabric defect detection algorithms

2.3.2.1. Spatial Methods

In spatial approaches, the features extracted are based on the spatial distribution of gray values [26]. Ideally, the statistical parameters of defect-free areas of the fabric will remain constant while those of areas with defects will be varying and/or will take different values.

One of the simplest methods that fall into this category is bilevel thresholding. The received signal will present sudden, instantaneous spikes or falls when a defect with high contrast is encountered. One research has employed this method to detect defects in real time [27]. Another fabric inspection system [28] that utilizes thresholding, followed by noise removal, followed by local averaging has succeeded in the detection of eight different types of defects. These systems, along with others that use bilevel thresholding [29] [1], are easy to implement but fail to detect defects that only slightly change the statistical parameters of the area they are in. An example is show in Figure 2.2.

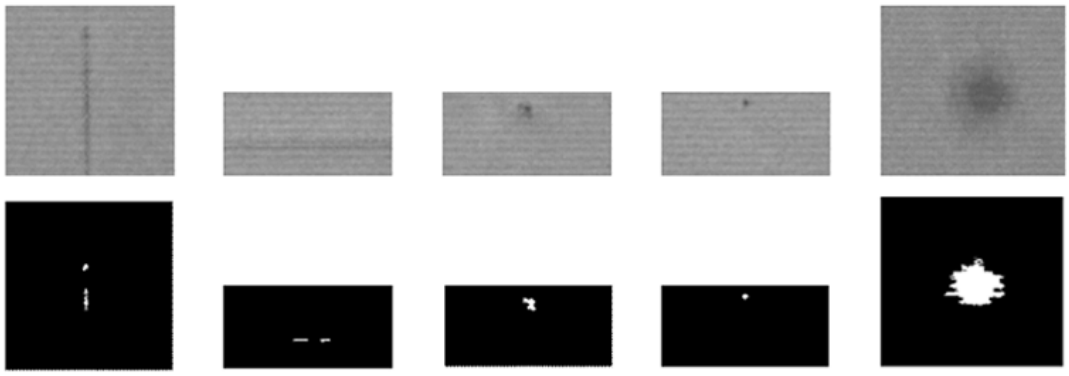

Figure 2.2: Fabric defect detection using bilevel thresholding [1]. All defects appear as dark patches/lines on the light-coloured fabric. Notice how most of the defect in (b) is not detected due to its tapering ends not being adequately dark.

The most common defects in fabrics such as holes, oil spots, colour flies and dirty yarn (Figure 2.3) stand out because of the differences in intensity between the defect and the fabric. Due to this fact, edge detection algorithms have been

used to isolate defects. The number of gray level transitions in the image leads to multiple spatial discontinuities in the fabric image such as lines, edges and point defects. These have been used as the features that define a defect in some research. A U.S. patent outlines a methodology to detect defects by transforming the fabric image to a set of masks, thresholding to separate the defect pixels, dilating to remove noise and finally carrying out blob analysis [30]. The Sobel edge detector has been used in one research but the methodology has not been described [31]. However, it compares their algorithm with using fractal dimensions to extract textural features. These methods have the disadvantage of being sensitive to the noise that arises from the fabric structure and therefore are likely to give false alarms for the detection.

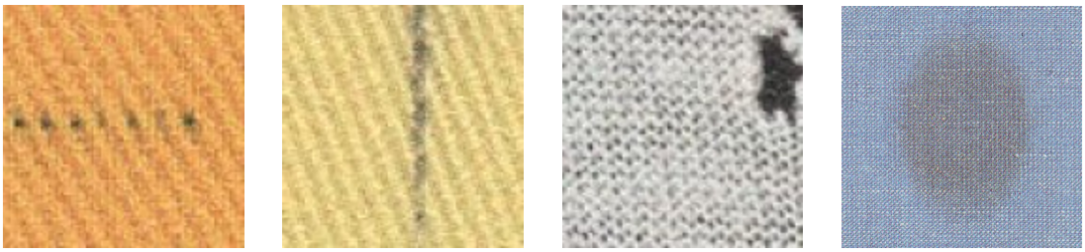

Figure 2.3: Defects from left to right: Colour Fly, Dirty Yarn, Hole, Oil Spot

Methods involving the gray level matrices, especially the Gray Level Co-occurrence Matrix (GLCM), are popular for texture analysis. Researchers have attempted to detect non-uniformities in the texture occurring due to defects by using these methods. Researchers have used two [32] or four [33] of the 14 features that can be derived from the co-occurrence matrix. A system that can detect defects as small as 1 mm squared has also been proposed in a paper [34] and it claims a detection rate of 95%. For the GLCM to be used in texture anomaly detection, the parameter θ should be in the orientation of the fabric pattern and the distance parameter d should be equal to the pattern period. The two prominent problems in this approach are that it ignores the spatial relationship between texture patterns and that it is sensitive to image noise [35].

Local linear transforms such as the Discrete Cosine Transform (DCT), Discrete Sine Transform (DST) and the Discrete Hadamard Transform (DHT) have also been used for feature extraction in fabrics. The performance of DCT, DST, DHT and Laws masks (filtering the image with different masks to give discriminative information) for fabric defect detection have been compared in [36]. However, their dataset only comprised two types of defects and therefore does not provide information of how well it would generalize to a larger number of defects. Another research paper [37] has used 5 x 5 Laws masks on 10 x 10 windows of the image to extract ripple, edge and weave features from the image. These features are subsequently used for the classification of each 10 x 10 window into defective or defect-free images by using a neural network. The advantage of using local linear transforms is that DCT or DST can be directly obtained from the camera using commercially available chips that optimize the speed and efficiency of the transforms. Thus, these methods might prove to be useful in real-time systems.

Local Binary Patterns (LBP) uses the gray level of the centre pixel of a sliding window as a threshold for the neighbouring pixels. This feature of LBP operators make them suitable for texture analysis. The features extracted are the statistics of the integer labels after the image has been transformed by the LBP operator. A few research [2] [38] [39] has been done on using LBP operators for detecting defects. LBP methods are computationally simple and invariant to grayscale changes. However, they are not invariant to rotation and as the LBP only considers the difference in pixel intensities, the magnitude of the intensities are ignored. This might be disadvantageous as some defects, such as holes, dirty yarn and oil spots, can be easily detected by their high intensity gray levels. To make the algorithm more flexible, Tajeripour et al. [38] and Fu et al. [2] have used modified LBP operators for defect detection. One LBP operator used by the latter is shown in Figure 2.4 and the results are shown in Figure 2.5.

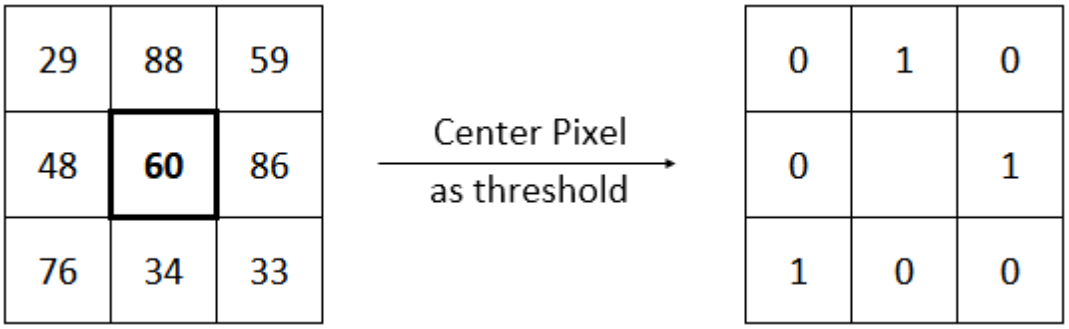

Figure 2.4: Adaptive Local Binary Pattern (ALBP) on a square neighbourhood [2]

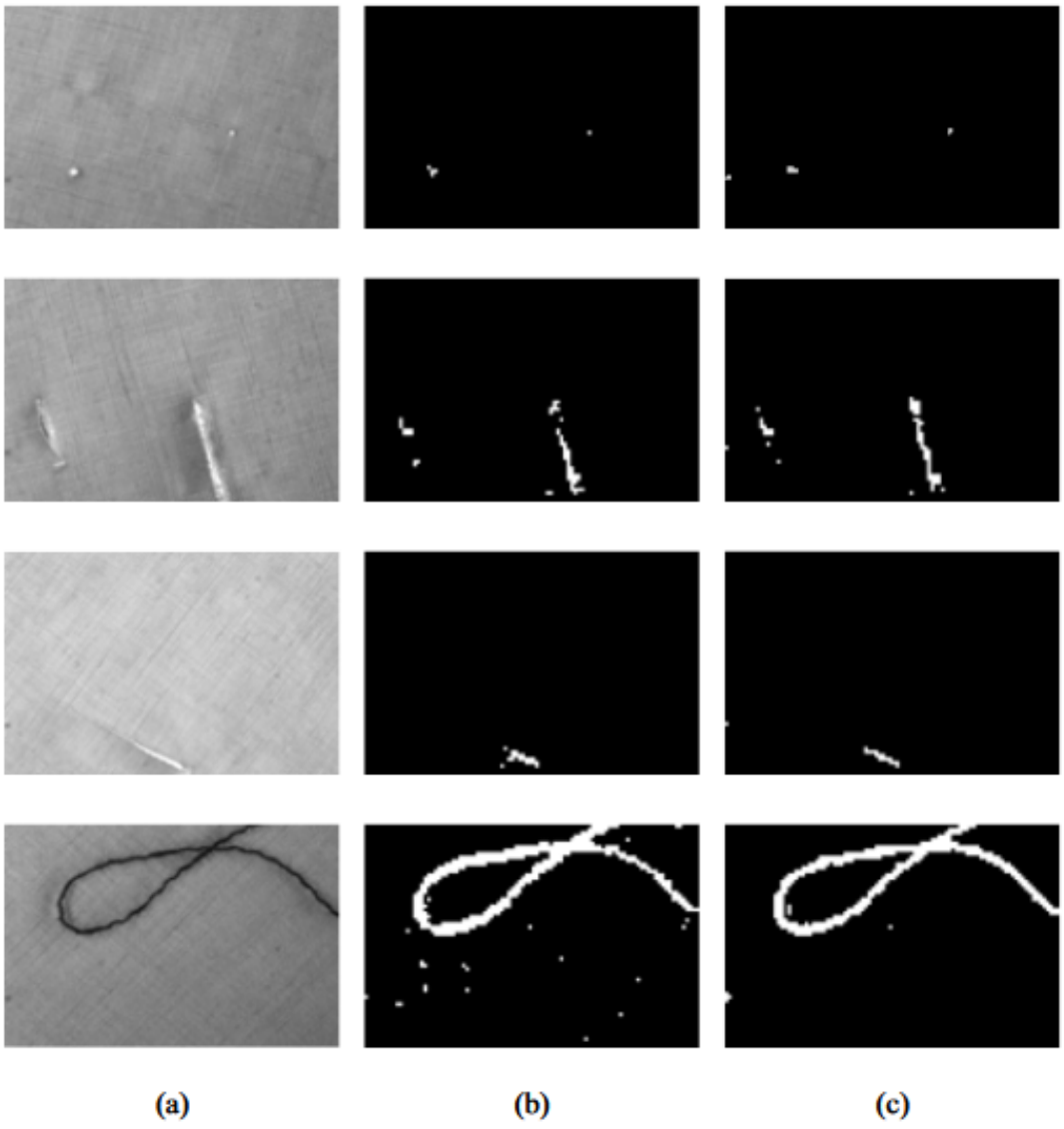

Figure 2.5: ALBP used on defective images. (a) original images, (b) images with 3x3 ALBP operator on 8x8 non-overlapping windows of the image, (c) images with 5x5 ALBP operator on 16x16 non-overlapping windows of the image [2]

Table 2.1 shows a comparison of the most common spatial methods used in fabric defect detection.

Table 2.1: Advantages and disadvantages of spatial methods

Spatial Approach	Advantages	Disadvantages
Bilevel thresholding	Easy to implement	Poor results when the intensity transition is gradual
Edge detection	Good for plain weaves	Sensitive to noise arising from the fabric structure
Gray level matrices	Small defects can be identified	Sensitive to noise arising from the fabric structure
Neural networks	Generalization capability	The absence of a good dataset
Local binary patterns	Computationally simple, invariant to illumination changes	Only the difference in pixel intensities are considered

2.3.2.2. Spectral Methods

Owing to the high degree of periodicity of yarns in fabrics, spectral approaches are suited for detecting anomalies in the fabric texture. The spectral features of a defective fabric image will, ideally, be distinct from a defect-free fabric image. In literature, features in the spatial-frequency have been used for defect detection. These features have the added benefit of being less sensitive to noise. The main objective of these approaches is to extract texture primitives and model or generalize the spatial placement rules [16].

Fourier transforms can be applied to monitor the spatial frequency spectrum of the fabric because faultless fabric is a repetitive and regular global texture. The occurrence of a defect causes this regular structure to change such that the corresponding intensity at some specific positions of the frequency spectrum will also change with it. Sari-Sarraf and Goddard [40] have used the Discrete Fourier Transform (DFT) to monitor the yarn density of a fabric and ensure that it meets the required quality standard. In this research, the spectral values inside several annular regions in the frequency spectrum are operated on to obtain a 1-D signature. The statistics of this 1-D signature are used to characterize the fabric

in terms of yarn density. Tsai and Huang [41] has presented a method that relies on the global reconstruction scheme using the Fourier transform. They have obtained the frequency spectrum of the image and applied a circular threshold to remove the frequencies corresponding to the repetitive features, thus, isolating the spectrum of the defective region. Tsai and Hu [42] have succeeded in presenting the Fourier models of four different kinds of fabric defects — missing end, missing pick, broken fabric and oil stains. A combination of DFT and the Hough transform has been used by Tsai and Heish [3] for the detection of defects in fabrics with directional textures. The Hough transform has been used to detect the high-frequency components of the DFT-transformed image. On suppressing certain frequencies of the image, it is reconstructed using the inverse DFT to obtain the defective regions. An example is shown in Figure 2.6

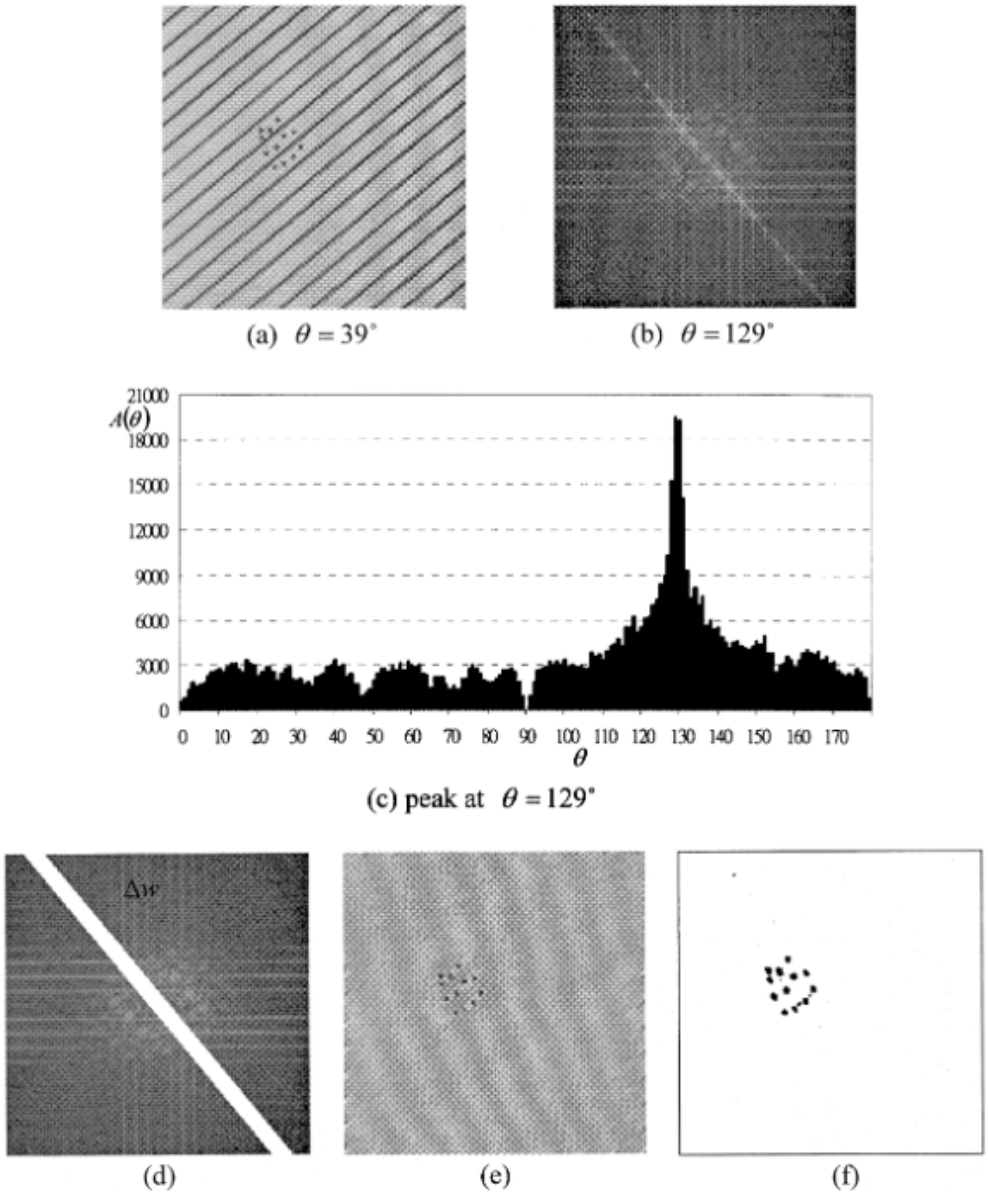

Figure 2.6: A line-structural texture with dot-spot defect: (a) the original image: (b) the Fourier domain image: (c) the slope-angle histogram in the Hough space:(d) the notch that contains high-energy frequency components with frequencies manually set to zero: (e) the restored image: (f) the detected dot spots displayed as a binary image. [3]

DFT cannot be used when the spatial localization of defects is also needed. Moreover, as the DFT is applied globally, small defects might not be detected by

the feature estimation process for the large region. To overcome these problems, the Windowed Fourier Transform (WFT) has been used by researchers. In a research by Campbell and Murtagh [43], a 16 x 16 window is used to extract the amplitude spectrum using the WFT. The same process is used to extract features from the defect-free sample and the classification of a fabric as defective or defect-free is done using a statistical hypothesis test. Feature extraction and binary classification using a hypothesis test has been done in a similar way in two other sources [44] [45].

The repetitive structure in fabrics can have small deviations in the production process and these deviations can be detected as defects in Fourier transform techniques. These deviations are actually not defects and therefore lead to a large number of false positives. Partly owing to this drawback, researchers have turned their attention to Gabor filters. Gabor filters can be used to represent both the spatial and frequency components of the images. Many researchers have extracted the texture features that represent the frequency content of the localized regions by using localized spatial filtering [46] [47] [48] [46]. The tunable parameters of Gabor filters are highly advantageous as they can be customized to detect a specific category of defects. Another characteristic of a Gabor filter is that its real part acts as a blob detector. This characteristic has been used in describing the process of texture segmentation by using Real Gabor Functions (RGF). A bank of multi-orientation and multi-solution RGF and subsequently, intra- and inter-scale image fusion has been utilized for the segmentation of defects in a few research [49] [50]. However, multi-resolution decomposition results in redundant features at different scales.

The redundant features at different scales when using a bank of Gabor filters is a result of the unorthogonality of the Gabor functions. This can be avoided by using orthogonal or biorthogonal wavelets to decompose the image to several scales. Wavelets possess the additional benefit of being shift-invariant. A system that can detect defects as small as 0.2 in has been developed by Sari-Sarraf

and Goddard [59] using the Daubechies wavelet for the transform. Their overall approach is shown in Figure 2.7. They claim to have achieved an overall detection rate of 89%. Some researchers [19] [51] [52] [53] have succeeded in defect detection by obtaining the energy and the entropy of the wavelet transform. If statistics based on the energy and entropy are above a certain threshold, the fabric has been classified as defective or defect-free. Applying the wavelet transform repetitively to obtain several layers of subimages can be done in two ways — wavelet tree decomposition and wavelet packet decomposition. Researchers have used both methods for multilayer decomposition. Packet decomposition results in more features due to the many subimages it creates when compared with tree decomposition but the question whether these additional features make a difference remains to be seen. A comparison study [53] states that the GLCM and wavelet analysis combined are likely to produce better results than either one alone. It is also stated that the decomposition of the image to more than three levels may cause defect information to be lost [54]. Backpropagation neural networks were supplied with the features extracted from the wavelet-transformed images in some research [55] [56] [57] [58]. The maximum number of defects detected in this approach is seven [58]. Wavelets, like Gabor filter functions, can be tuned to detect a specific category of defect. Three customized wavelets are used by [59] to detect four kinds of defects that commonly appear in Denim fabrics. A modified signal-to-noise ratio formula has been used as the criteria for classification. Researchers have attempted to overcome the inability of wavelet functions to detect defects with smooth grayscale differences by designing new wavelets with the lifting scheme [4]. However, the results are shown only for a small number of defects. A patented system [60] has used the wavelet transform to extract spatial-frequency features and then performed a feature vector reduction based on a Fuzzy rough decision set. The tradeoff in this method is that when a small number of features are selected, defects cannot be effectively identified and when a large number of defects are identified, the real-time performance and real-time accuracy is reduced.

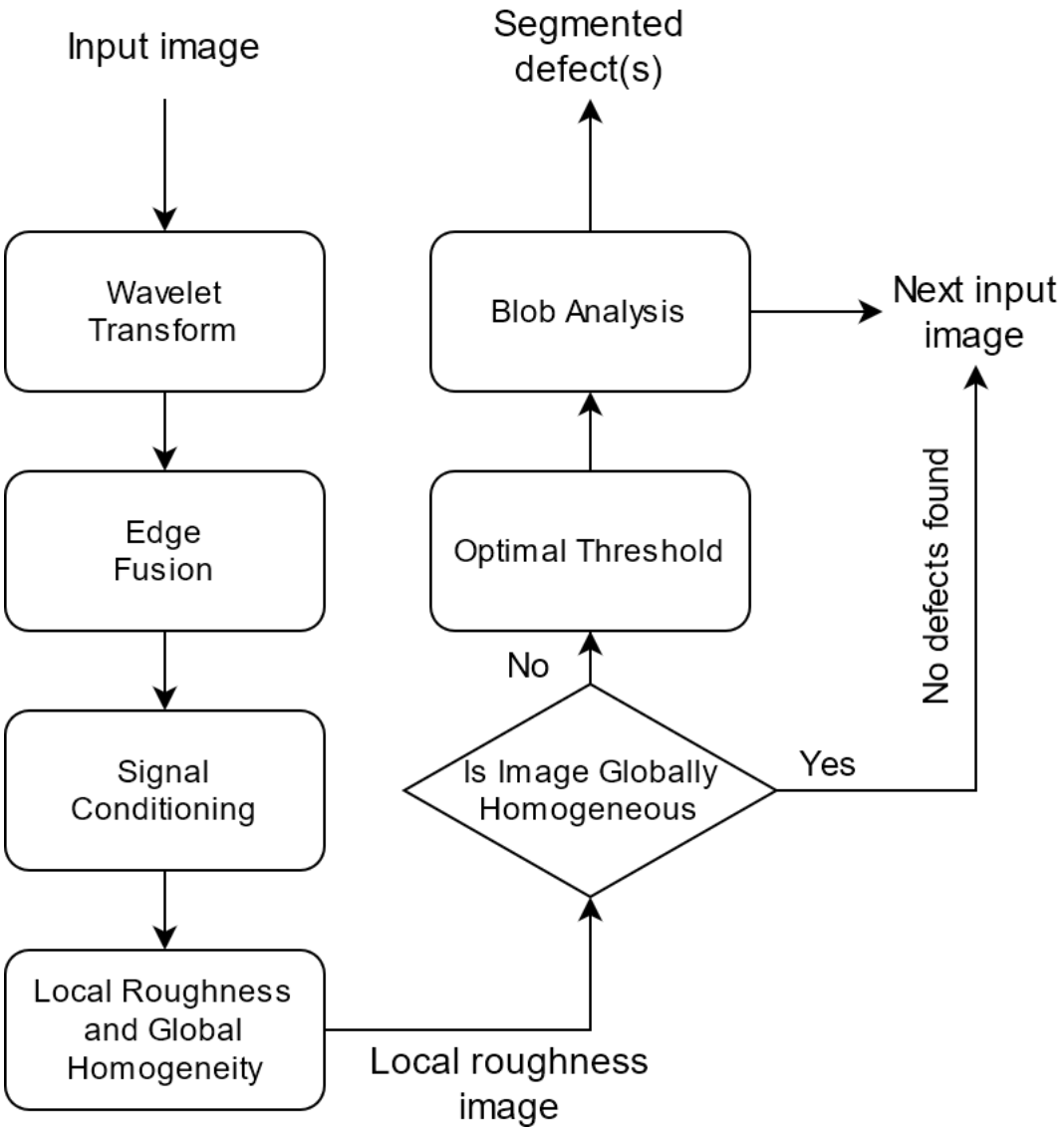

Figure 2.7: Wavelet-based scheme for the detection and segmentation of fabric defects [4]

Table 2.2 shows a comparison of the most common spectral methods used in fabric defect detection.

2.3.2.3. Model-based Methods

Texture can be defined as a deterministic or stochastic model [14]. However, real-world textures have a combination of deterministic and stochastic compo-

Table 2.2: Advantages and disadvantages of spectral methods

Spectral Approach	Advantages	Disadvantages
Discrete Fourier Transform (DFT)	Noise immunity. Translation invariance. Good at detecting global defects	Spatial information is lost. Some local defects might go undetected.
Windowed Fourier Transform (WFT)	Spatial information is preserved. Good for local defects	Not good at detecting global defects
Gabor filters	Tunable. Contains both spatial and frequency information	Computationally complex. Cannot meet real-time speeds
Wavelet transform	Less computationally complex. Shift-invariant. Tunable	Performs poorly on flat defects with smooth grayscale differences

nents. Real textures can be modelled as stochastic processes and textured images can be observed as realizations or samples from parametric probability distributions on the image space [61]. A few probabilistic models of the textures have been proposed by researchers for fabric defect detection.

Cross and Jain [62] have shown that stochastic models based on the Gauss-Markov Random Field (GMRF) model successfully represent many natural and synthetic textures. Cohen et al. [63] have used a method where the defect-free fabric is modelled from the parameters of training samples. When a test fabric is introduced, it is separated into blocks and a chi-squared test is used to determine if the fabric is defective or defect-free. The GMRF model is used in a much similar way in [64], [61] and [65]. After a comparison study, Attali and Cohen [66] have suggested that Markov-random-field-based methods are well-suited for modelling fabric textures than fractal models, which excel at modelling perceptual surface roughness. Brzakoviæet al. [67] [68] have proved that the modelling of randomly textured surfaces are possible using Poisson's model. Even though it was not implemented for fabrics, they have shown that the difference between predictions from the theoretical model and actual measurements was as low as 10%.

Model-based clustering assumes that the data were generated by an unknown model and tries to recover the original model from the data [69]. Faint aligned defects have been detected using this method by Campbell et al [70]. The Bayesian information criterion has been used to classify the fabric as defective or defect-free in their paper. A colour clustering algorithm has been employed in Kong et al.'s research [71]. An initial K-means clustering and a subsequent perceptual merging is done to detect images of defective fabrics. As the technique heavily relies on colour information, it is provides poor results for gray fabrics.

Fabric defect detection can be presented to a neural network in the form of a binary classification problem. Neural networks are good classifiers because of their robustness, adaptive learning, generalization capability and self-organization. In [72], the feature vector has been extracted based on the gray level of each pixel and principal component analysis has been used to reduce the number of dimensions. The reason for the extraction of a gray-level based feature vector is that defects in the fabric alter the gray levels of the surrounding pixels. A low-cost fabric defect detection system has been proposed in [73] using linear neural network. Real-time detection has also been achieved using neural networks in [74]. The features, in this case, have been extracted using the local binary pattern texture operator and the self-organizing map. Backpropagation neural networks have been used extensively in defect detection after feature extraction by a variety of methods including fuzzification [75], wavelet decomposition [55], [56] and edge detection [76]. Recently, Convolutional Neural Networks (CNN) and deep CNNs have attracted the attention of researchers. Jing et al. [77] have input labelled patches of the image into a pretrained CNN for transfer learning and the system was able to detect defects during the testing phase by sliding the whole image over the trained model. A major setback in using neural networks for fabrics is the absence of a sufficiently large dataset. To surmount this obstacle, Mei et al. [78] has used a multi-scale convolutional denoising autoencoder. Image patches are reconstructed at multiple Gaussian pyramid levels. Weninger et al. [79] have used a fully-convolutional network to track individual yarns. This is then used

to make a grid of the criss-cross structure of the woven fabric. Once the grid is obtained, deviations of the grid points from the ideal structure will point to a defect. Li et al. [80] have extended this approach to patterned fabrics using Fisher-criterion deep learning using stacked denoising autoencoders. The variety of neural networks available for classification remains a promising avenue for further research in defect detection.

2.3.3 Defect Classification Methods

Defect classification refers to the process of categorizing the defect into a defect class e.g. hole, thick place, burl, slub etc. It follows defect detection. Identifying the class of the defect enables the fabric manufacturer to trace the origin of the defect to a manufacturing subprocess and subsequently take steps to rectify the error. If the defects are detected and classified by a garment manufacturer, the information is conveyed to the supplier as part of their quality assurance process.

2.3.3.1. Statistical Inference

A simple method of classifying defects is from the statistics of the features extracted from the fabric image. Jiang et al. [52] have extracted two features (peak energy, peak entropy) from each layer of a two-layer wavelet decomposition of the image. They have then categorized a defect as a warp defect, weft defect, oil stain or hole based on the eigenvalues. Behravan et al. [81] have employed local binary patterns for defect localization and to classify the defects, they have used a filter bank on textons. Textons are certain microstructures such as spot-like features, bar-like characteristics and edges with different orientations that are said to be the underlying cause for human texture perception [82]. A filter bank introduced by Leung and Malik [83] which consists of the first and second derivatives of the Laplacian of Gaussian filters was used to analyze the texture in order to classify the defect. Li et al. [84] have used Estimating Signal Parameter

via Rotational Invariance Technique (ESPRIT) for extracting spectral features from patterned fabric. The subsequent classification is done using a rough set classifier by taking into consideration a total of 16 features of the flaw area. A success rate of over 90% has been reported. Vladimir et al. [85] have used morphological operations to obtain the contours of the defects. Classification of the defects into seven categories have been accomplished by obtaining the statistics of the contours' geometric features such as the average area. A similar approach has been taken by Mottalib et al. [86] where the geometric features obtained have been categorized using a simple Bayesian classifier. They claim to have classified six types of defects with a 95% accuracy. They have suggested a reduction in the number of features by combining multiple features for future work. Even though statistical approaches are relatively simple, the existence of multiple types of defects that give similar statistics are a limiting factor

2.3.3.2. Support Vector Machines

Support Vector Machines (SVM) are frequently-used algorithms for classification problems because they are effective in higher dimensional spaces i.e. when the number of dimensions exceed the number of samples.

Murino et al. [87] have extracted three sets of features. The first set is from the histogram of the grayscale image, the second is a set of geometric features derived from the shape of the defect and the third consists of features from the co-occurrence matrix. To extend the capability of a SVM for a multivariate classification, a 1-vs-1 binary decision tree scheme has been used. Up to 11 defects have been classified in this manner. A research on using the LBP operator to extract features from colour images in different colour spaces have been conducted by Hoang and Rebhi [88]. The subsequent classification has been accomplished by using a one-vs-all SVM classifier. An accuracy of 92.1% has been achieved in the luminance-chrominance colour space. Basu et al. [22] have used principal component analysis on blocks of the image to extract features that represent the

local variation of pixel intensities. When coupled with a SVM classifier and tested on the TILDA fabric defect database, an accuracy of 96.36% has been achieved. Two patents [89] [90] have also been published on SVM-based classification. One [89] uses Gabor convolutional filtering with an optimized Gabor filter for feature extraction and a subsequent single-class SVM classifier, while the other [90] has used the wavelet transformation to obtain features, a Fuzzy rough decision set for feature reduction and a SVM for classification. The use of a single-class SVM for the former has the claimed advantages of avoiding problems like over-learning, under-learning and local extrema. A real-time performance has been achieved by the both systems.

Although SVMs are robust classification algorithms and perform well for classification problems involving a higher number of dimensions, they can be computationally expensive due to the expensive five-fold cross validation needed for calculating probability estimates.

2.3.3.3. Neural Networks

The defect classification method that is most used in research are artificial neural networks. Due to their non-linear nature and ability to learn patterns in fabric defects, they are popular among researchers involved in classification problems. Neural networks have the added benefit of learning to classify previously unseen defects, if a training phase is incorporated into the system. A major drawback in using neural networks in the textile industry is the absence of an adequately large dataset because the size of the dataset has a direct impact on the performance of the network in the validation process. However, some variations of neural networks have been especially designed to work with frugal datasets and they might be suited for the problem in question.

The backpropagation algorithm has been one of the most commonly used algorithms for training a neural network. The iterative, gradient-descent algorithm

makes it an efficient method of updating weights as new data in provided as input. Backpropagation neural networks have been used for defect classification in many research [15] [91] [55] [56] [5]. Su et al. [55] have used the wavelet transform for feature extraction and a backpropagation neural network for classification. The Taguchi method has been used to improve the efficiency of the neural network. A classification accuracy of 96.5% has been achieved for four distinct types of fabric defects. Liu and Qu [56] have also employed the wavelet transform to decompose the image into 3 resolution levels. Gray level statistics were calculated from the resulting images, which were fed into the neural network. The use of images in several resolutions has provided a larger feature set which has the potential to classify a larger number of defects but the paper only discusses the identification of 3 types only. Islam et al. [5] has used geometric features obtained after thresholding to feed into the neural network but has achieved lower accuracies, proving that geometric features alone are not good descriptors of defects. The neural network architecture they have used is shown in Figure 2.8

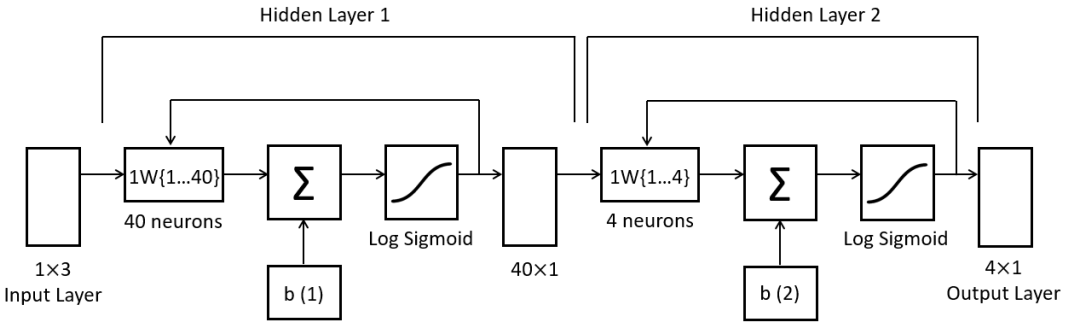

Figure 2.8: A typical backpropagation neural network used in defect detection [5]

Learning Vector Quantization (LVQ) networks are a special type of neural network that lets the designer choose the training instances that the network should focus on learning. LVQs are fairly interpretable and therefore sound decisions can be made when making modifications without resorting to trial and error. Liu and Zuo [92] have compared the classification capabilities of LVQ neural networks with both spatial and spectral features. The spatial features has given a higher

classification accuracy but this may be due to the large number of spatial features that have been used compared to the smaller number of spectral features.

An adaptive neuro-fuzzy inference system has been used by Venkatesan et al. [93] However, the classification algorithm has not been described. Four features computed from the gray-level co-occurrence matrix in four orientations were used. An accuracy of 100% has been reported for 2 types of defects and their combination.

2.4 Summary

The various techniques used for fabric defect detection and classification in previous studies have been reviewed in this section. The strengths and weaknesses of the most commonly-used methods have also been compared. Taking into account the imperfections in each method, the past studies conducted using multiple methods, and the conclusions of past surveys on defect detection methods, it can be seen that using a combination of multiple methods is likely to yield better detection and classification accuracies when compared to using a single method. The next section uses this insight gained about fabric defect identification to develop a methodology.

Section 3
Methodology

This section describes the basis on which the feature extraction algorithms were selected, the feature extraction algorithms themselves and the classifiers used for defect detection.

A typical image processing pipeline built for image classification has three main components. They are preprocessing, feature extraction and classification as shown in Figure 3.1. As a multimodal approach is followed in this research, multiple feature extraction algorithms are used. The preprocessing performed on the images were integral and specific to each feature extraction algorithm. Hence, the preprocessing steps are described as part of the feature extraction pipeline in Section 4, rather than being described separately.

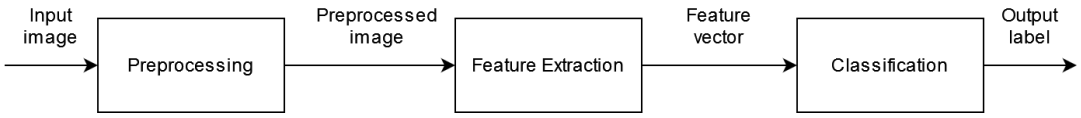

Figure 3.1: General architecture of an image processing pipeline for image classification

3.1 Selection of feature extraction algorithms

The algorithms chosen for preliminary investigation in this research were thresholding, the gray-level co-occurrence matrix (GLCM) and the wavelet transform. These algorithms were chosen based on the literature according to two criteria — the algorithms that have been used to classify the most number of defects and the algorithms that have classified defects with the most accuracy. Figure 3.2 shows

the number of defects that have been successfully classified by each technique and Figure 3.3 shows the number of defects that each technique has classified with the highest accuracy. It should be noted that these data have been acquired from research on fabric defect identification i.e. detection and classification both.

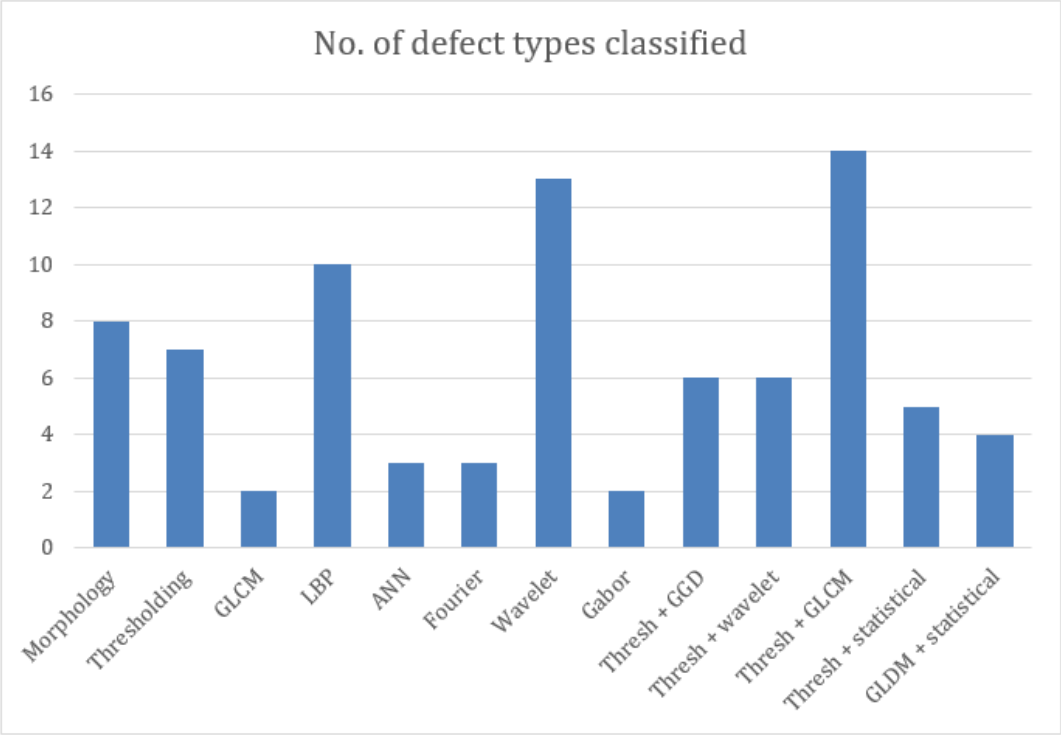

Figure 3.2: Number of defects classified by each technique in past studies

It is clear that the wavelet transform is the unimodal technique that has classified the most number of defects with the highest accuracies and has classified the second largest number of defects (13). The multimodal technique that has combined bilevel thresholding and the GLCM has been successful in classifying the most number of defects (14) and has classified a reasonable number of defects with the highest recorded accuracy. It is because of these two reasons that these algorithms have been chosen as a starting point in this research.

In addition to the performance of these algorithms in prior research, they can be used to obtain a set of distinct features that are able to describe the image in

multiple domains. Thresholding is performed in the spatial domain and is one of the few techniques that can extract geometric features such as area, perimeter, height, width etc. from the defect area. Defects can be broadly categorized quite easily if these features are obtained. However, isolating the defect using thresholding alone has proven to be difficult, because defects which do not alter the mean gray level of the defect-free region go undetected. Therefore, thresholding has been replaced with local entropy feature extraction in this research.

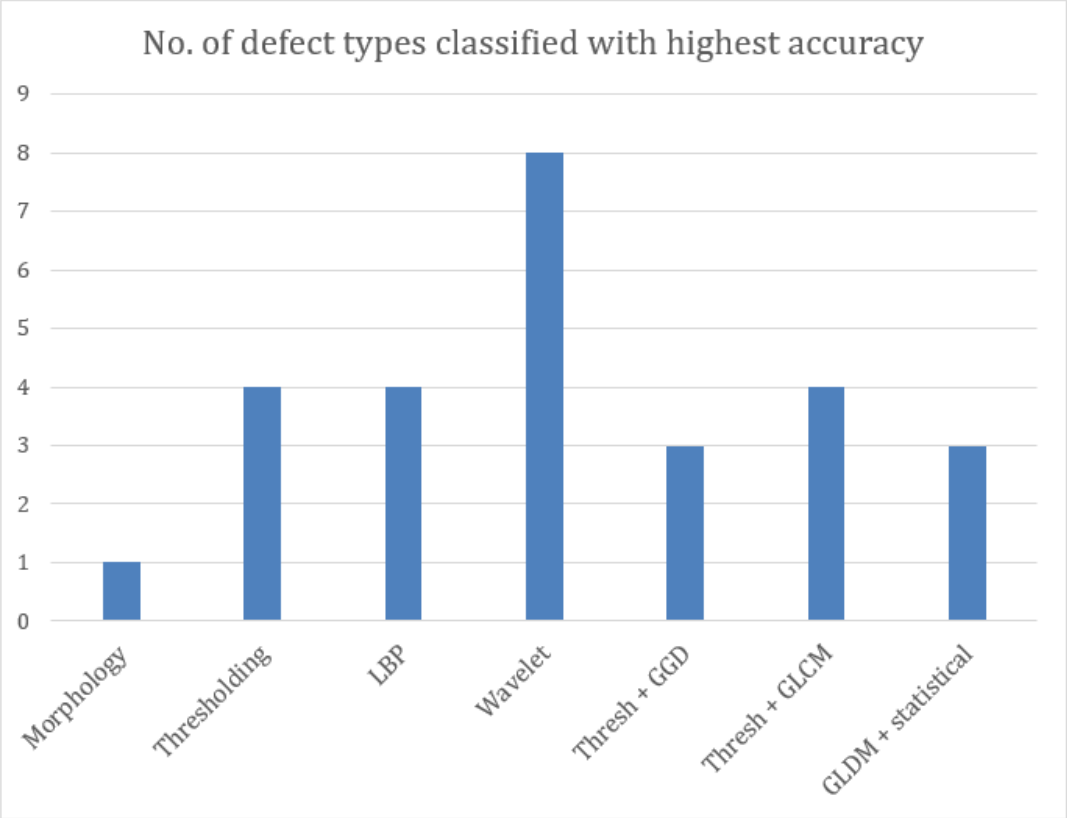

Figure 3.3: Number of defects classified with the highest accuracy by each technique in past studies

The GLCM is a popular texture descriptor as it can extract a total of 14 textural features from an image. As defects will disrupt the pattern of yarn in the fabric, these features will differ in defective fabrics when compared to defect-free ones. Investigation of the variation of these features for different types of

defects will be useful in determining if certain features of the GLCM are sensitive to certain types of defects. An alternative method of using this technique is to use the co-occurrence matrix itself as a feature, without computing the textural features. It has also been proved that the GLCM can be used to detect defects as small as $1mm^2$ [34]. The problem with using GLCM alone is that the spatial relationship between texture patterns will be ignored. This will be problematic when localizing the defective area in the fabric. The GLCM has also been known to be sensitive to noise in the image, which, in this case, will be the noise arising from the structure of the fabric itself such as stray fibres in the yarn.

Wavelet transforms are widely used for feature extraction in image processing due to its low sensitivity to noise. This feature of wavelet transforms coupled with the capability of wavelets to be tuned to detect a specific type of defect makes this method the most prolific in both defect detection and classification studies. Owing to the significant number of studies on defect identification with wavelets, most variations of the wavelet transform have already been tested. These include decomposing the image up to three levels, using both wavelet packet and tree decomposition, transforming the image with multiple wavelets and sometimes even using the transform and its inverse as a preprocessing step to remove noise. Decomposing the image to multiple levels with the two decomposition techniques will enable the extraction of features in multiple resolutions and wavelet transformation using multiple wavelets enable the differentiation of the defects that respond to different wavelet frequencies. The energy and the entropy of the transformed image are the two features that have been used in the classification studies that have succeeded in classifying up to 8 features [94] [95].

3.2 Dataset Used

Our dataset was created as follows. From the 195 512x512-pixel images in the publically available Cotton Incorporated dataset [96], the images of unpatterned

fabrics containing Abrasion Mark, Broken End, Broken Pick, Burl, Coarse End, Coarse Pick, Colour Fly, Dirty Yarn, Dropped Stitches, Foreign Yarn, Hole, Knot, Missing Yarn, Oil Spot, Slub, Thick Place and Thin Place were selected. For the purpose of generalizing the approach for a wide variety of fabric, 46 different types of fabric representing both woven and knitted fabrics were included. They were randomly cropped with a 128x128 window and annotated with the support of domain experts. The resulting dataset consisted of 3084 images, of which 1700 are defective and 1384 are defect-free. Sample images of each defect and their details are shown in Table 3.1.

When training the classifiers, 2202 images were taken as the training set. These 2202 images comprised 990 defect-free images and 1212 defective images. The testing set comprised 882 images, of which 394 were defect-free and 488 were defective.

Table 3.1: Types of defects in the dataset

Defect type	**Description**	**Severity**	**Example image**
Abrasion mark	Scuffing or abrasion of the fabric	Major	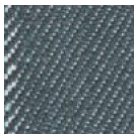
Broken end	Excess yarn woven into the filling as a result of a broken warp end	Major	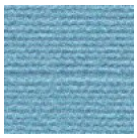

Table 3.1: Types of defects in the dataset

Broken pick	Absent weft yarn	Major	
Burl	Result of a pulled-out slub	Major	
Coarse end	Result of a warp end that is larger than normal	Major	
Coarse pick	Result of a weft yarn that is larger than normal	Major	
Colour fly	Small amounts of coloured fibre, accidentally woven in.	Major	
Dirty yarn	Oily, dirty or greasy yarn	Major	

Table 3.1: Types of defects in the dataset

Dropped stitches	Stitches failing to form due to a malfunctioning needle.	Major	
Foreign yarn	Other yarn interwoven with the desired yarn	Major	
Hole	An opening in the fabric created by one or more damaged yarns	Major	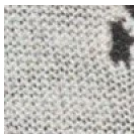
Knot	Broken yarn pieced together	Minor	
Missing yarn	Result of the machine continuing to run with one yarn broken/missing	Major	

Table 3.1: Types of defects in the dataset

Oil spot	Stain made by oil dropped on the fabric	Mostly minor	
Slub	Thick place in the yarn caused by flying waste yarn	Mostly minor	
Thick place	Yarn diameter is larger than normal in a region.	Major	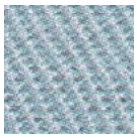
Thin place	Yarn diameter is smaller than normal in a region	Major	

3.3 The Gray-level Co-occurrence Matrix

Texture can be thought of as a spatial variation of the gray level intensities in an image. Hence, an examination of the spatial dependencies between the grayscale pixel intensities will result in a quantification of the image's texture. Following this line of reasoning, the concept of the GLCM was developed and

extensively used in texture analysis [97] [98] [99] [100].

The GLCM can be defined as follows: Given a grayscale image with Q gray levels, the GLCM is a Q × Q matrix, where the number of occurrences of dipoles with gray levels i and j are recorded at (i,j) in the matrix shown in Figure 3.4. A dipole is defined as a pair of pixels that are D pixels apart in a direction, θ as shown in Figure 3.5. The GLCM can be normalized, in which case each element in the matrix becomes the probability of a dipole's occurrence in the image. It has been shown that features calculated from the GLCM of an image can be used as reliable texture descriptors [26]. These features are also called the second order statistics of the image.

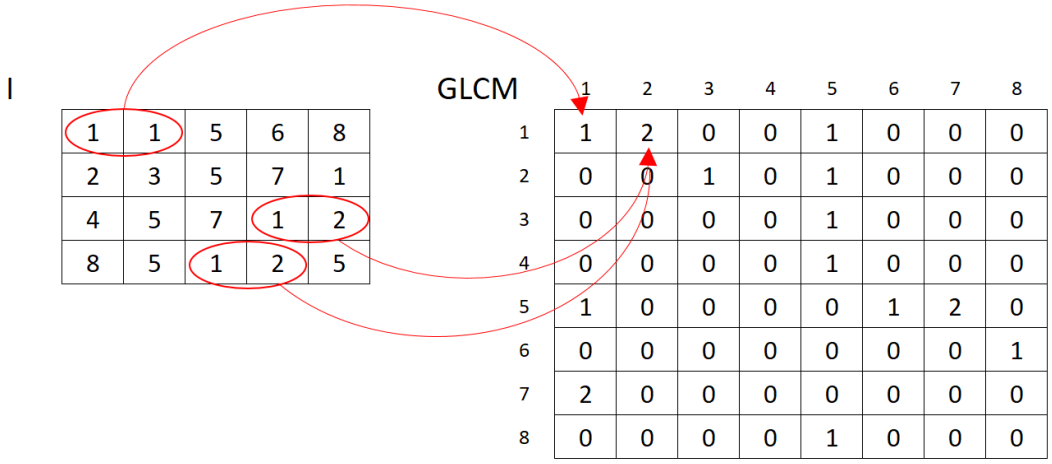

Figure 3.4: Construction of the GLCM with D = 1 and $\theta = 0°$

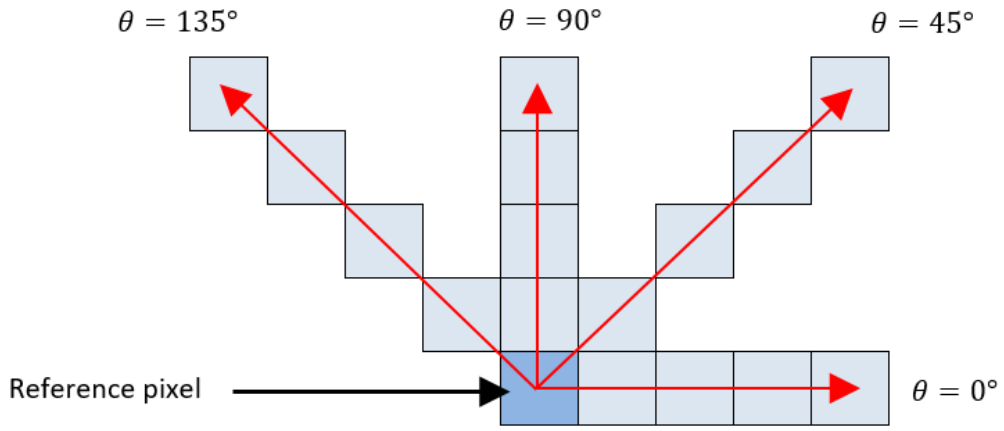

Figure 3.5: 4 possible directions (θ), for D = 4

3.4 The Discrete Wavelet Transform

The DWT is used to represent a function by a sequence of coefficients. It is similar to the Fourier transform. One major difference between the Fourier transform and the wavelet transform lies in their use of basis functions. Where the Fourier transform uses trigonometric functions as the basis, the wavelet transform uses a family of bases generated by combining a wavelet function (ψ), as in formula 3.1, and a scaling function (ϕ), as in formula 3.2 also known as the mother and father wavelets, respectively.

$$\psi_{m,k}(x) = \psi(2^m x - k) \tag{3.1}$$

$$\phi_{m,k}(x) = \phi(2^m x - k) \tag{3.2}$$

where $m, k \in \mathbb{Z}$ and control the dilation and the translation of the functions. The other difference between the two is that even though the Fourier transform

characterizes the frequency distribution of the images, it does not consider the information in the spatial domain and tends to ignore local deviations in frequency [101] [41] [102], unlike the wavelet transform, which preserves spatial information while providing frequency information.

The preferred method of efficiently computing the wavelet coefficients is by using an iterative filterbank of low pass (L) and high pass (H) filters derived from the scaling and wavelet functions, followed by a signal downsampling step. For a 2D signal, such as an image, the filters are passed along the rows and then the columns to obtain one low-resolution approximation image (LL) containing the low frequency components and three detail images containing the high frequency components. One detail image (HL) contains the vertical edges, one contains the horizontal edges (LH) and the other, the diagonal edges and corners (HH). This decomposition of the image is commonly represented as a dyadic partition of a rectangle, called a subband pattern as seen in Figure 3.6.

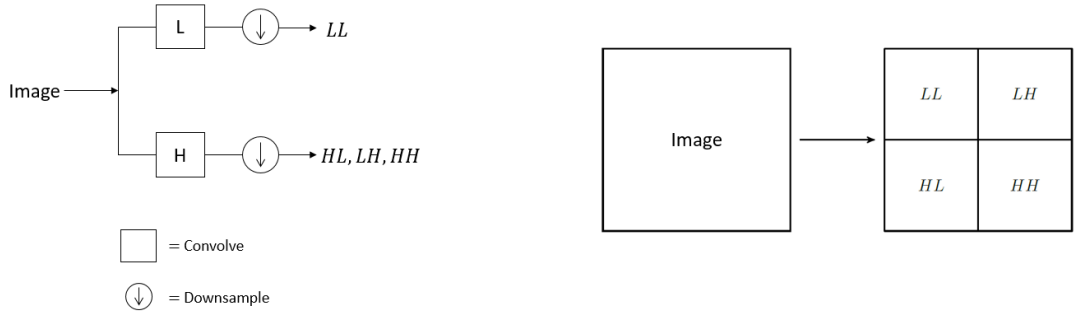

Figure 3.6: Filterbank representation of the wavelet transform (left) and the subband pattern (right) for one pass of the filterbank

To further extract the high frequency components, the iterative filterbank may be applied to the approximation image and/or the detail images. Repeated application of the filterbank to the approximation image only, is known as Mallat decomposition, while repeated application of the filterbank to all sub-images is known as packet decomposition. These two methods of decomposition are shown in Figure 3.7. Each application of the filterbank is called a level of decomposition.

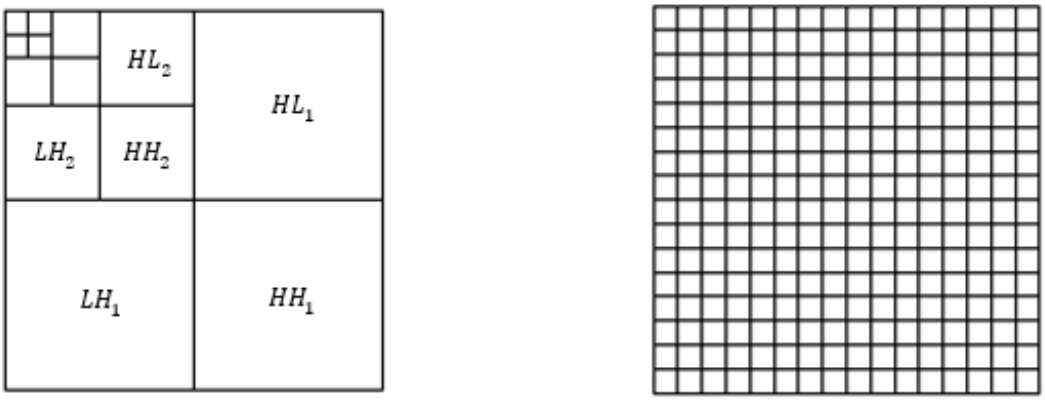

Figure 3.7: Mallat (left) and packet (right) decomposition to four levels

The feature used to quantify the edge content of each sub-image is the energy, defined by equation 3.3.

$$Energy = E = \sum_{i=0}^{M} \sum_{j=0}^{N} H_{i,j}^2 \tag{3.3}$$

where M and N are the number of rows and the number of columns of the image array, respectively, and $H_{i,j}$ is the intensity of a pixel at row i and column j. As the sub-images are binary, the edge content of the sub-image is quantified by the energy. Past studies [51] [55] [52] [95] [103] have proven that the energy of a sub-image can not only be used to ascertain the existence of a defect, but also to determine the type of defect, given that the range of defects in question is small. The energies of HL, LH and HH for each level of decomposition are taken as the wavelet features in this research.

3.5 Local Entropy

The local entropy at a pixel in an image is a measure of the randomness of the gray level distribution in a neighbourhood around it. The local entropy tends

to fluctuate less for the pixels of a defect-free image, as the uniformity of the texture throughout the image maintains an approximately constant gray-level distribution around all pixels. The presence of some defects causes the gray-level distribution around the defect to deviate from the expected and thus the local entropy near the defect is much higher or much smaller compared to the rest of the image. Some defects that are subtle but occupy a large area in the captured image do not result in a single spot in the image to have abnormally high or low entropy values. However, they tend to increase the variance in the overall local entropy distribution in the image.

The entropy of each pixel at (i,j) in a (2n+1)×(2n+1) neighbourhood is given by the following equation:

$$H(i,j) = -\sum_{p=i-n}^{i+n}\sum_{q=j-n}^{j+n} P(p,q)log(P(p,q))S(p,q) \tag{3.4}$$

where $P(i,j)$ is the intensity of the pixel at (i,j) and $S(i,j)$ is the value of the structuring element at (i,j).

In this research, the local entropy at each pixel in a disc-shaped neighborhood in computed. The local entropy map obtained thus is used to determine the standard deviation of the local entropy distribution in the image.

3.6 Classification Algorithms

Since the classification accuracy significantly depends on the type of classifier, the performance of five algorithms on the dataset are compared. The k-NN, random forest, multi-layer perceptron (MLP), support vector machine (SVM) and Naïve-Bayes classifier are selected as they are commonly-used in feature-based classification problems of this nature. Each classifier has been trained with

five-fold cross-validation and a grid search is carried out beforehand to select the best parameters for each algorithm.

3.7 Summary

In this section, the data gathered and the conclusions inferred from the literature review has been used to develop a methodology for fabric defect identification. Three algorithms have been selected to extract features from the fabric images. The three algorithms were selected based on the highest performing algorithms that have succeeded in identifying a considerable number of defects. Each of these algorithms are described in this section.

The features extracted from the combination of these algorithms are then input to a classifier. The selection of the five classifiers chosen for this task has also been described. Apart from these, a brief description of the seventeen types of defects used in this study are tabulated.

In the following section, the algorithms chosen are optimized to suit the problem at hand.

Section 4

Feature Extraction and Defect Identification

This section describes the complete feature extraction and defect identification process. An overview of the approach is shown in Figure 4.1. Each segment of the approach is described in the subsections below.

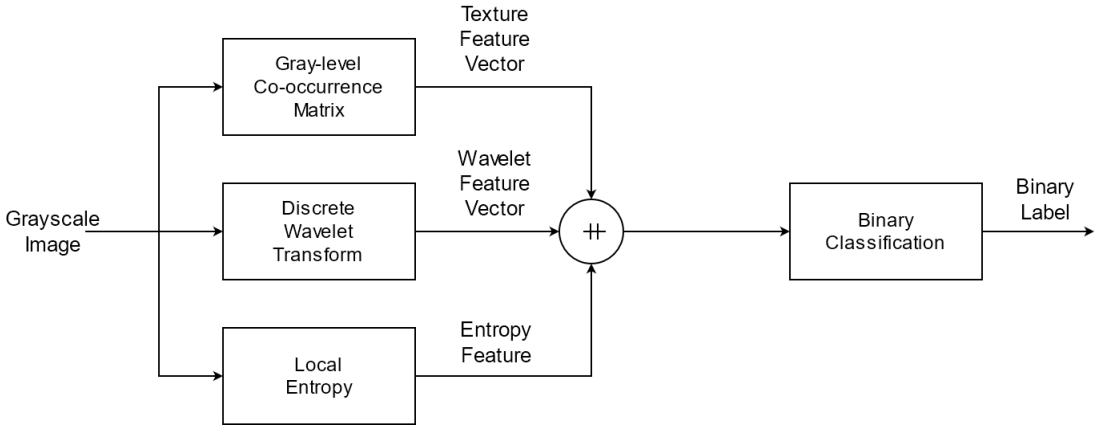

Figure 4.1: Overview of the approach

4.1 Texture Feature Extraction

Texture feature extraction refers to the process of quantifying the texture of a fabric. Texture features are significant in defect detection because the presence of defects distorts the normal texture of the fabric. In this research, the GLCM is selected for extracting texture features.

4.1.1 Selection of offset, orientation and features

A total of 14 features were introduced in the original paper [26], out of which three are regarded as the least correlated [104] [105] [106]. These three features are the energy (ENE), contrast (CON), correlation (COR). Apart from these features, homogeneity (HOM) and entropy (ENT) have also been widely used for texture analysis with good results [107] [97]. Formulae 4.1 – 4.5 show the calculation of these features from the GLCM, where $P_{i,j}$ is the element of the GLCM at (i, j) and $levels$ is the number of gray levels in the image.

$$ENE^2 = \sum_{i,j=0}^{levels-1} P_{i,j}^2 \tag{4.1}$$

$$CON = \sum_{i,j=0}^{levels-1} P_{i,j}(i-j)^2 \tag{4.2}$$

$$HOM = \sum_{i,j=0}^{levels-1} \frac{P_{i,j}}{1+|i-j|} \tag{4.3}$$

$$ENT = -\sum_{i,j=0}^{levels-1} P_{i,j}\log(P_{i,j}) \tag{4.4}$$

$$COR = \sum_{i,j=0}^{levels-1} P_{i,j}\frac{(i-\mu_i)(j-\mu_j)}{\sqrt{\sigma_i^2\sigma_j^2}} \tag{4.5}$$

where μ_i, μ_j, σ_i and σ_j are calculated from formulae 4.6 - 4.9:

$$\mu_i = \sum_{i,j=0}^{levels-1} i(P_{i,j}) \tag{4.6}$$

$$\mu_j = \sum_{i,j=0}^{levels-1} j(P_{i,j}) \tag{4.7}$$

$$\sigma_i^2 = \sum_{i,j=0}^{levels-1} (P_{i,j})(i - \mu_i)^2 \tag{4.8}$$

$$\sigma_j^2 = \sum_{i,j=0}^{levels-1} (P_{i,j})(j - \mu_j)^2 \tag{4.9}$$

Energy can be used to distinguish between homogeneous images and images with random tonal variations. As the intensities of the pixels in homogeneous images will result in a GLCM with a few, but large, values, energy will be greater in those than in images with random tonal variations, where the GLCM will not be as sparse, but will contain smaller values (Figure 4.2).

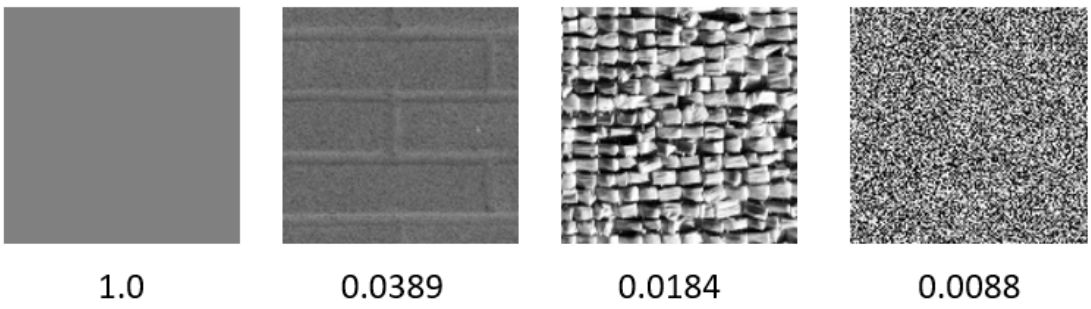

Figure 4.2: Energy computed from the normalized GLCM

Contrast is proportional to the amount of local intensity variations of the image and will be greater when pixels have similar and larger changes in intensity (Figure 4.3). Homogeneity has an inverse correlation with contrast.

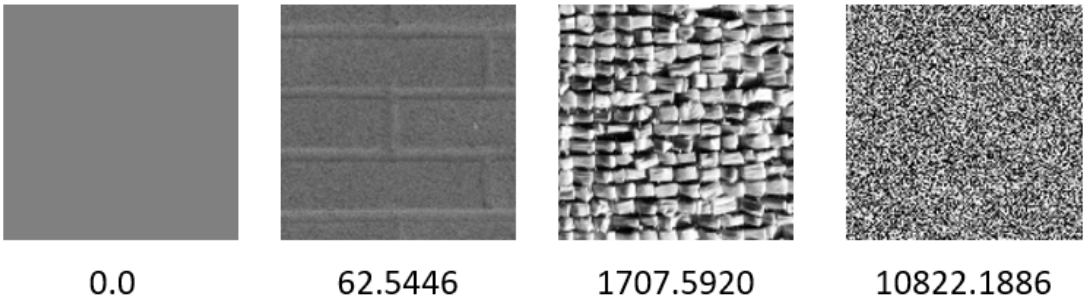

Figure 4.3: Contrast computed from the normalized GLCM

Correlation measures the gray-tone linear dependencies of the image. If the correlation is computed for a moving window on the image, it will show significant change when there is a change in the texture (Figure 4.4).

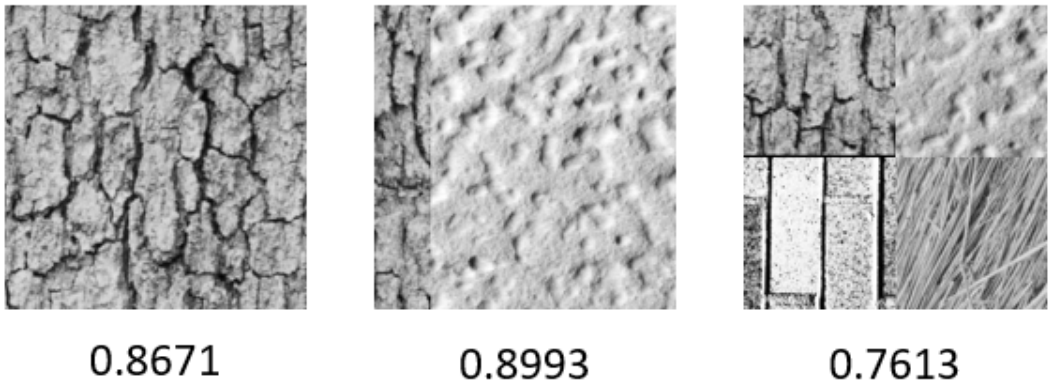

Figure 4.4: Correlation computed from the normalized GLCM

Entropy has a strong inverse correlation to energy and is therefore greater when there are many tonal variations in the image (Figure 4.5).

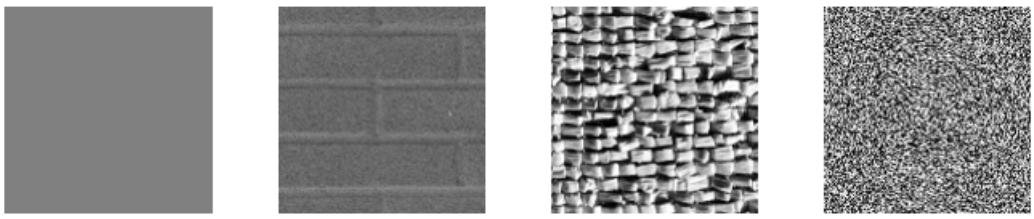

Energy	1.0	0.0389	0.0184	0.0088
Entropy	0.0003	0.2925	0.6189	0.8869

Figure 4.5: Energy and entropy computed from the normalized GLCM

ENE,CON,COR,HOM and ENT are taken as the textural features in this research. The dipole length (D) and orientation (θ) should, ideally, capture the period of the texture. Image texture varies depending on the resolution of the captured image, or for a human observer, the distance at which the fabric is observed. In a very high resolution image of a fabric, the texture will be a result of the structure made by interlaced yarn. In a low-resolution image, the texture will arise due to variations in colour and printed patterns, if any. Therefore, it can be said that the perceived texture of a fabric is dependent on the resolution of the image.

This research uses both woven and knit fabrics and due to the changeable nature of the structure of some knit fabrics, the period of the texture may change in certain locations in the fabric. Moreover, a period cannot be inferred in fabrics that have a silky texture and the presence of many strands of yarn sticking out in cotton and wool fabrics makes the discerning of a period more difficult (Figure 4.6). Tests on images with multiple resolutions and a variety of textures with unpredictable periods have revealed that a dipole length of 1 is a reasonable choice for most textures [108] [109]. As for θ when the typical texture orientation cannot be inferred, the GLCMs for each of the four possible orientations, 0°, 45°,

90°and 135°are computed and the average of each feature computed from each GLCM is taken [26] [106]. This causes a significant increase in computational cost, but is necessary to obtain a reliable texture descriptor.

Figure 4.6: Wavy knit fabric (left), satin fabric of uniform colour (middle) and wool fabric (right)

4.1.2 Optimization of window size and gray level bit depths

In order to determine the optimal window size and the number of gray levels that the image should be reduced to, an experiment to detect defective images using the five selected GLCM features was conducted. As previously mentioned, the reason for this experiment was the lack of a consensus on the best window size and number of gray levels due to these being heavily dependent on the dataset being used.

The experiment shown in Figure 4.7 involves comparing the texture feature vector of a query image (image to be labelled) to that of a reference image. In order to test the performance on multiple window sizes and multiple levels of gray level quantization, textural features were extracted from the same image with four different window sizes (8x8, 16x16, 32x32, 64x64) and six different gray levels (8, 16, 32, 64, 128, 256).

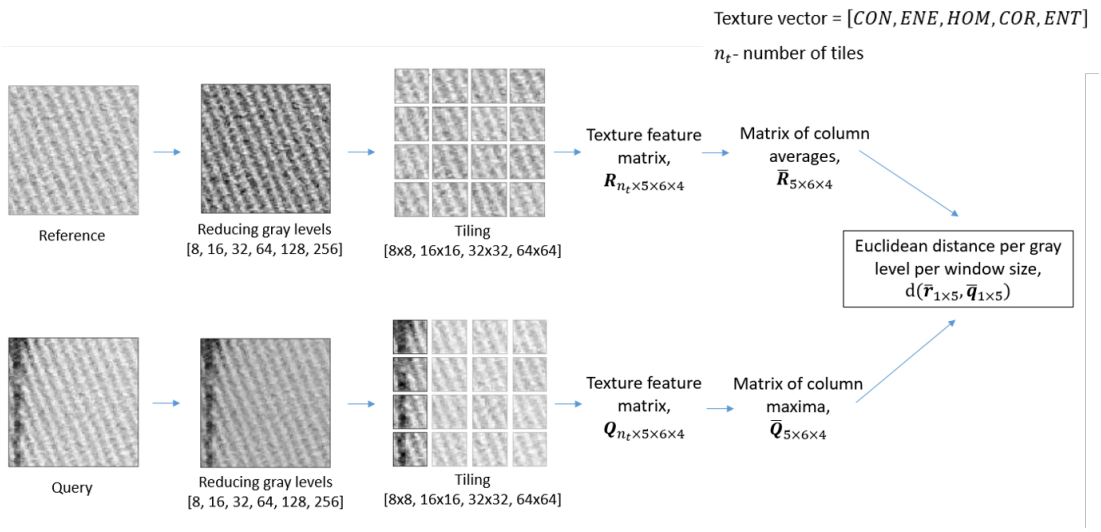

Figure 4.7: Experiment to select the optimal window size and gray level bit depth for the GLCM

Since the image should be considered defective if even one tile has a distortion in texture, the maximum of each texture feature was extracted from the tiled query image as its texture vector. This feature vector is compared to the vector of texture feature averages extracted from the reference image, using the Euclidean distance as the dissimilarity metric. If the Euclidean distance is above a threshold, the query image is labelled defective. In the initial stage of the experiment, the detection was performed in an unsupervised manner — the query image and the reference image were one and the same. To elaborate, given a query image, the vector of textural feature maxima of the image was compared with the vector of textural feature averages of the same image. The second stage of the experiment is a supervised approach, where the reference image is a defect-free template image. In the practical scenario, before the algorithm runs, the inspector would provide the machine with a defect-free area of the fabric to be inspected.

4.1.3 Summary of Findings

Initial unsupervised detection led to poor performance, evidently because of global defects that propagate across a major portion of the image. Supervised detection, with a separate template image for each fabric type, led to higher accuracies. An analysis of the results showed that 8 gray levels and a 16x16 window size yielded the best detection accuracies. The results are presented and discussed in more detail in subsection 5.2.1.

4.2 Spectral Feature Extraction

Spectral feature extraction refers to the process of extracting features from an image converted to the frequency domain from the spatial domain. Spectral features are important in detecting defects in fabrics with periodic textures because some defects disrupt the periodicity of the texture. The discrete wavelet transform is used in this research to convert the image into the frequency domain.

4.2.1 Selection of wavelet function and mode of decomposition.

It has been shown that fabric texture usually occupies the intermediate range of the frequency spectrum, while the majority of fabric defects occupy the high-end [110]. So, the ideal wavelet function would be one that can capture only those frequencies which correspond to the defect. However, as the choice of a single wavelet function that can filter out the variety of different textures available in the dataset is not possible, a function that would capture both the fabric texture and the defect has been used in this research. The existence of a defect is determined by a significant change in the energy of one of the sub-images.

In order to choose the mother wavelet, the ones used in prior texture analysis research were noted (Table 4.1).

Table 4.1: Mother wavelets used in research articles

Research article	Mother wavelet used
29 30 16 31 32 33 34	Daubechies
29 18 35 28	Haar
36	Coiflet
29	Symlet

Haar wavelets have been shown to be unable to efficiently separate image signals into low and high frequency subbands. Furthermore, they do not respond to sharp transitions in the signal [111]. A comparison between Haar and Daubechies (*db*) wavelets with more than one vanishing moment has revealed that *db* wavelets have continuous derivatives that respond well to discontinuities in texture [111]. Coiflets and symlets were only used in two studies, in which their performance can either be matched or surpassed by the *db* wavelet family. Due to these reasons, the *db* wavelet has been used for the wavelet transform in this research.

When choosing a *db* wavelet, the number of vanishing moments is an important consideration. The higher the number of vanishing moments the less compact it is (Figure 4.8). It has been shown that a more compact wavelet can capture the finer details of texture [112]. Even though some research [113] [110] has shown that the impact of the number of vanishing moments in fabric defect identification is limited, prior research has used wavelets with two [53] [4], three [51] [103] or four [53] [92] to varying degrees of success. Therefore, the number of vanishing moments for the *db* wavelet used in this research has been determined through an experiment.

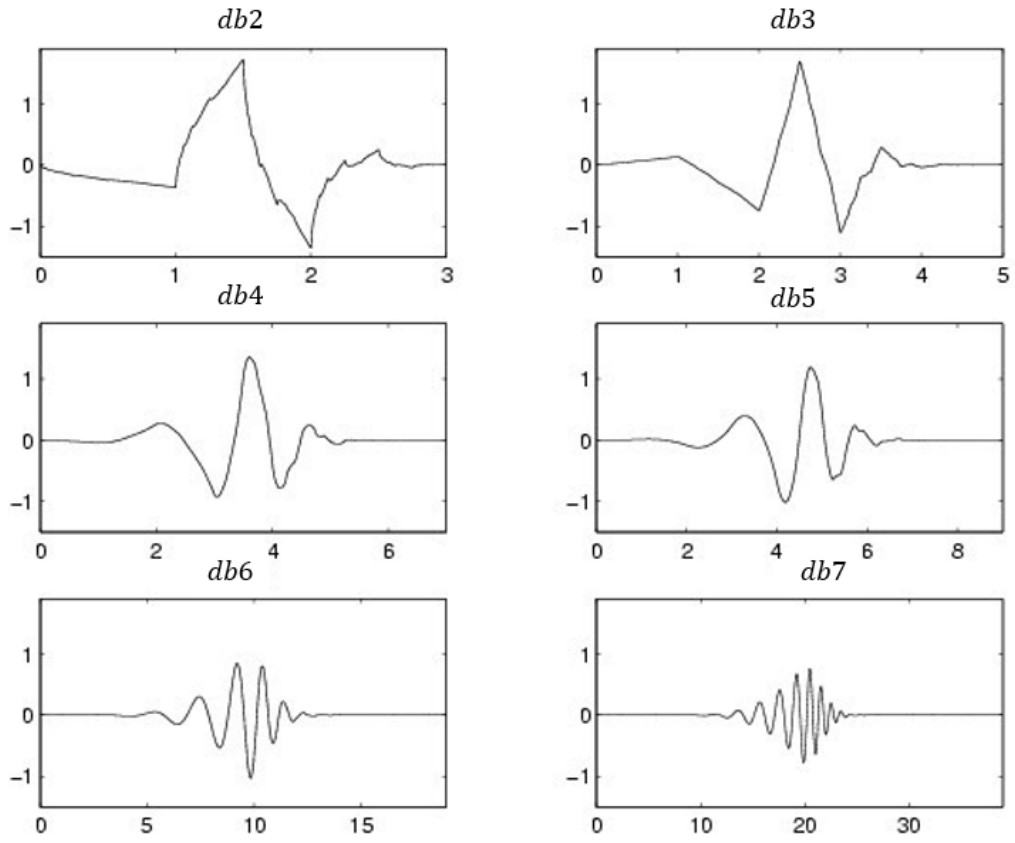

Figure 4.8: Daubechies (db) wavelets with different numbers of vanishing moments

It is evident through past research that some defects will be discerned more easily in higher levels of decomposition (Table 4.2), especially at the second or third level [110] [56]. However, using an excessive number of levels may result in the loss of small defects [113]. Most studies have concentrated on the analysis of 4 levels or less. One study [53] has adjusted the number of levels used based on the targeted defect type.

As a wide range of defects are chosen for detection in this research, an experiment was conducted to determine the best level(s) at which each defect was best identified.

The type of decomposition was chosen as Mallat decomposition. Packet de-

Table 4.2: Number of decomposition levels used in research articles

Research article	Number of decomposition levels used
[4] [51]	1
[110] [103] [114] [115]	2
[110] [51] [92] [56] [116] [117]	3
[113]	4

composition was not selected as the further application of the filterbank to the detail images have been shown to result in redundant features [53] [51] [115], which might have an impact on the classifier. Moreover, Mallat decomposition has been successfully used in many studies to achieve good detection accuracies [114] [116] [117] [103] [118] [110] [56].

4.2.2 Optimization of vanishing moments and levels of decomposition

Owing to the fact that the compactness of the wavelet function affects the high-frequency component extraction and the fact that different defects are more discernible in some levels of decomposition than others, an experiment was conducted to select the optimal number of vanishing moments and the levels of decomposition for this research.

The experiment 4.9 is similar to the one conducted in order to select the GLCM parameters. In this experiment, each image is subjected to the wavelet transform using three wavelets, $db2$, $db3$ and $db4$, which have vanishing moments of 2, 3 and 4 respectively. Only wavelets with a small number of vanishing moments were chosen because previous research had confirmed that the more compact a wavelet is, the better it can characterize finer texture [112], as mentioned previously. Each approximation image (LL) is then subjected to the wavelet transform two more times to achieve three levels of decomposition. The energies of each detail image (LH,HL and HH), E_H, E_V and E_D, corresponding to the horizontal, vertical and diagonal features, are extracted to form the wavelet feature vector corresponding to each level of decomposition.

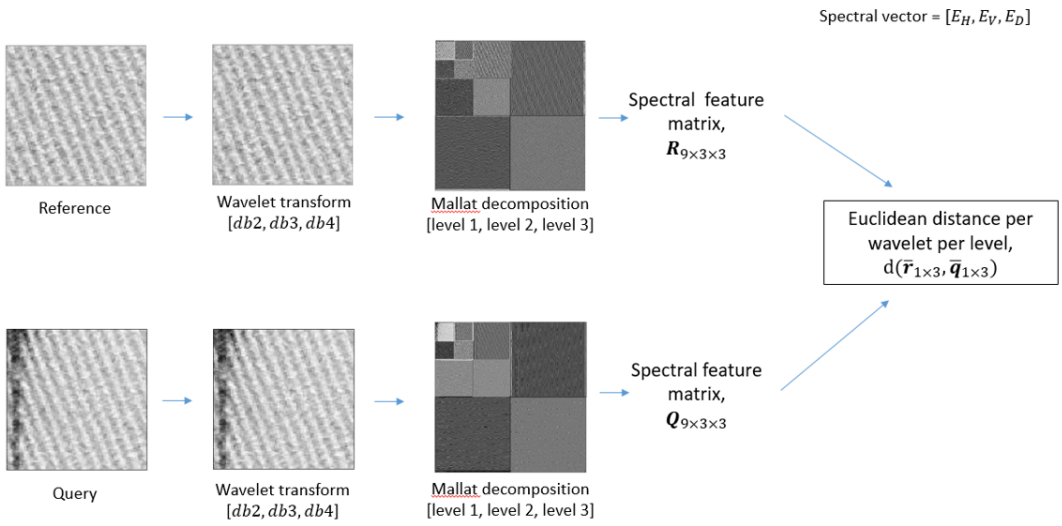

Figure 4.9: Experiment to select the number of vanishing moments and level of decomposition for the discrete wavelet transform

The wavelet features thus extracted are compared using the Euclidean distance and the query image is labelled as defective if it crosses a threshold, as before. The reference image used in this experiment is a defect-free template image and hence is a supervised approach.

4.2.3 Summary of Findings

Results of varying the number of vanishing moments showed that the db3 wavelet succeeded in detecting the most defects with the best accuracies. Interestingly, varying the levels of decomposition showed that there is no single level in which a considerable number of defects are detected with the best accuracy. Therefore, it was decided to extract spectral features from all three levels of decomposition. A graphical representation and detailed discussion of the results are given in subsection 5.2.2.

4.3 Entropy Feature Extraction

Prior to the feature extraction, each image in the dataset and in the set of reference images is subjected to a median blur using a 3×3 mask. A disc-shaped structuring element of radius 5 is placed on each pixel in the image and the local entropy per pixel is calculated. This results in the derivation of a local entropy map for each image as shown in Figure 4.10. In the figure, bluer pixels represent low entropies and yellower pixels represent higher entropies. The standard deviation of the local entropy distribution of each query image σ_Q and that of its respective reference image σ_R are calculated. The absolute deviation between these two values is taken as the local entropy feature vector of the query image as shown below in Equation 4.10.

$$\sigma = |\sigma_R - \sigma_Q| \tag{4.10}$$

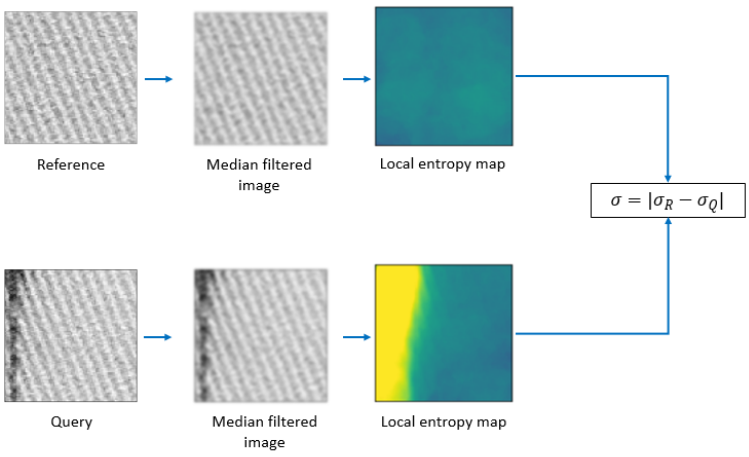

Figure 4.10: Local entropy feature extraction

4.4 Feature Ranking

Some features in high-dimensional feature spaces may carry non-discriminative or correlated information from the problem domain's perspective. These features do not contribute to the classifier performance and, in some cases, could even influence it negatively by biasing the classifier on directions outside the problem domain. Feature ranking determines the features which are most discriminative and relevant to a given classifier model.

In order to separate the feature ranking process from the classification, joint mutual information (JMI) [119] is used to rank features in this study. The classifier-independent features selected thus are generic. Additional advantages of using JMI are the lower chance of overfitting during classification and speed of computation [120] compared to classifier-dependent techniques. JMI is used from among other classifier-independent methods as it provides the best trade-off between accuracy and stability [121].

The mutual information I between two random variables, x and y is defined by Equation 4.11.

$$I(x:y) = \sum_{i,j}(p(x_i, y_j)log(\frac{p(x_i, y_j)}{p(x_i)p(y_j)})) \tag{4.11}$$

where p(x,y) is their joint probability density function and p(x) and p(y) are their respective marginal probabilities. When the mutual information is conditioned by a third variable z, it can be expressed by the Equation 4.12

$$I(x:y|z) = \sum_{k}(p(z_k))\sum_{i,j}(p(x_i, y_j|z_k)log(\frac{p(x_i, y_j|z_k)}{p(x_i|z_k)p(y_j|z_k)})) \tag{4.12}$$

The JMI score finds the feature that adds the most new information to a set

of already selected features ($f_j \in S$). The score is formulated for a feature under investigation (f_i) by Equation 4.13

$$JMI(f_i) = \sum_{f_j \in S} (I(f_i; c) + I(f_i; c|f_j)) \tag{4.13}$$

where c is the target class.

Detailed results of the feature ranking process are included in Section 5.2.3.

4.5 Defect Identification

The methods detailed in the above sections were used to extract a set of features that describe the textural, spectral and entropic information contained within the image. These features are then given as input to a classification algorithm to train it in separating defective fabric from defect-free fabric.

4.5.1 Defect detection

Since the detection accuracy significantly depends on the type of classifier, the performance of five algorithms on the dataset are compared. The k-NN, random forest, multi-layer perceptron (MLP), support vector machine (SVM) and Naïve-Bayes classifier are selected as they are commonly-used in feature-based classification problems of this nature. Each classifier was trained with five-fold cross-validation and a grid search is carried out beforehand to select the best parameters for each algorithm

4.5.2 Summary of Findings

Classification of the fabric images using the five classifiers showed that the k-NN achieved the best accuracy, whereas the random forest classifier came in second. The k-NN was used with 5 neighbours and the Manhattan distance. A closer look at the results showed that seven defects were classified with perfect accuracy, seven other defects were classified with very high accuracy and only three were classified with comparatively lower accuracy.

4.5.3 Summary

In this section, the selection of algorithm parameters using literature and experimentation are described. The offset, orientation and features to be computed from the GLCM are chosen based on past studies, whereas the number of gray levels and the window size are inferred through experiment. In the spectral feature extraction, the mother wavelet and the type of decomposition is chosen based on literature, whereas the number of vanishing moments and the levels of decomposition are selected through experimentation. The extraction of the local entropy feature is also described.

In the next section, the results of the experiments presented in this section are described in more detail with accompanying charts and graphs to visualize them.

Section 5

Results and Discussion

In this research, an algorithm is developed to detect defects in both knitted and woven fabrics. Features are extracted from each image using three techniques. The GLCM is used to extract five textural features, the discrete wavelet transform is used to extract nine spectral features and local entropy is used to extract one feature. These features are combined into a single feature vector and a binary classification is carried out to determine if a given image is defective or defect-free.

In this section, the results of the experiments that were conducted to determine the optimal parameters for the feature extraction algorithms are discussed. Subsequently, the results of the feature ranking are presented and lastly, the outcomes of the detection and classification of defects are explored.

5.1 Performance Metrics

The F1 score was used as the metric of choice because it balances the two metrics - precision and recall. Precision evaluates the performance of the classifier on the images it labels as positive (defective) and is penalized whenever an image is falsely classified as positive. Recall evaluates the performance of the algorithm on the actual defective images in the dataset and is penalized when a defective image is falsely classified as negative.

In the industry, the cost of missing a defect outweighs the cost of falsely detecting a defect. This is because the former causes heavy losses in garment production whereas the false positives in the latter can be identified in the subsequent gar-

ment cutting process. If a missed defect appearing in the finished clothing is detected in the final quality check, the clothing item may either be discarded or sold as a second quality garment in the local market with a % markdown in the price. If these defects are missed in the final quality check and are shipped to clients, the garment company risks a detrimental effect on their reputation because most large-scale garment manufacturers cater to high-value brands with rigorous quality standards. Due to these reasons, recall should be given the priority when analyzing classifier performance. However, evaluating the performance of the classifier solely on its recall is inadvisable as a perfect recall can be achieved by simply classifying all images as positive. For that reason, the precision of the classifier should not be ignored. Another reason for not ignoring precision is that too many false positives will be an inconvenience as it may lead to employees in later processes, such as garment cutting, taking time to look for the non-existent defects before making the cuts. Hence, the F1 score is used to evaluate the performance of the classifier in this research, as it is the harmonic mean of precision and recall.

$$Precision = \frac{TP}{TP + FP} \tag{5.1}$$

$$Recall = \frac{TP}{TP + FN} \tag{5.2}$$

$$F1Score = 2\frac{Precision * Recall}{Precision + Recall} \tag{5.3}$$

$$Accuracy = \frac{TP + TN}{TP + FP + TP + TN} \tag{5.4}$$

where TP is the number of true positives, TN is the number of true negatives, FP is the number of false positives and FN is the number of false negatives.

5.2 Experimental Results

The following subsections present the results of optimizing the textural and spectral feature extraction, followed by the results of feature ranking and defect detection. Each set of presented results is followed by a discussion.

5.2.1 Results of texture feature optimization

The F1 scores of the unsupervised detection with GLCM textural features were graphed, as shown in Figure 5.1. Each curve represents the average F1 score across all defect categories. The threshold for the Euclidean distance was varied over a range, in order to obtain the optimal threshold.

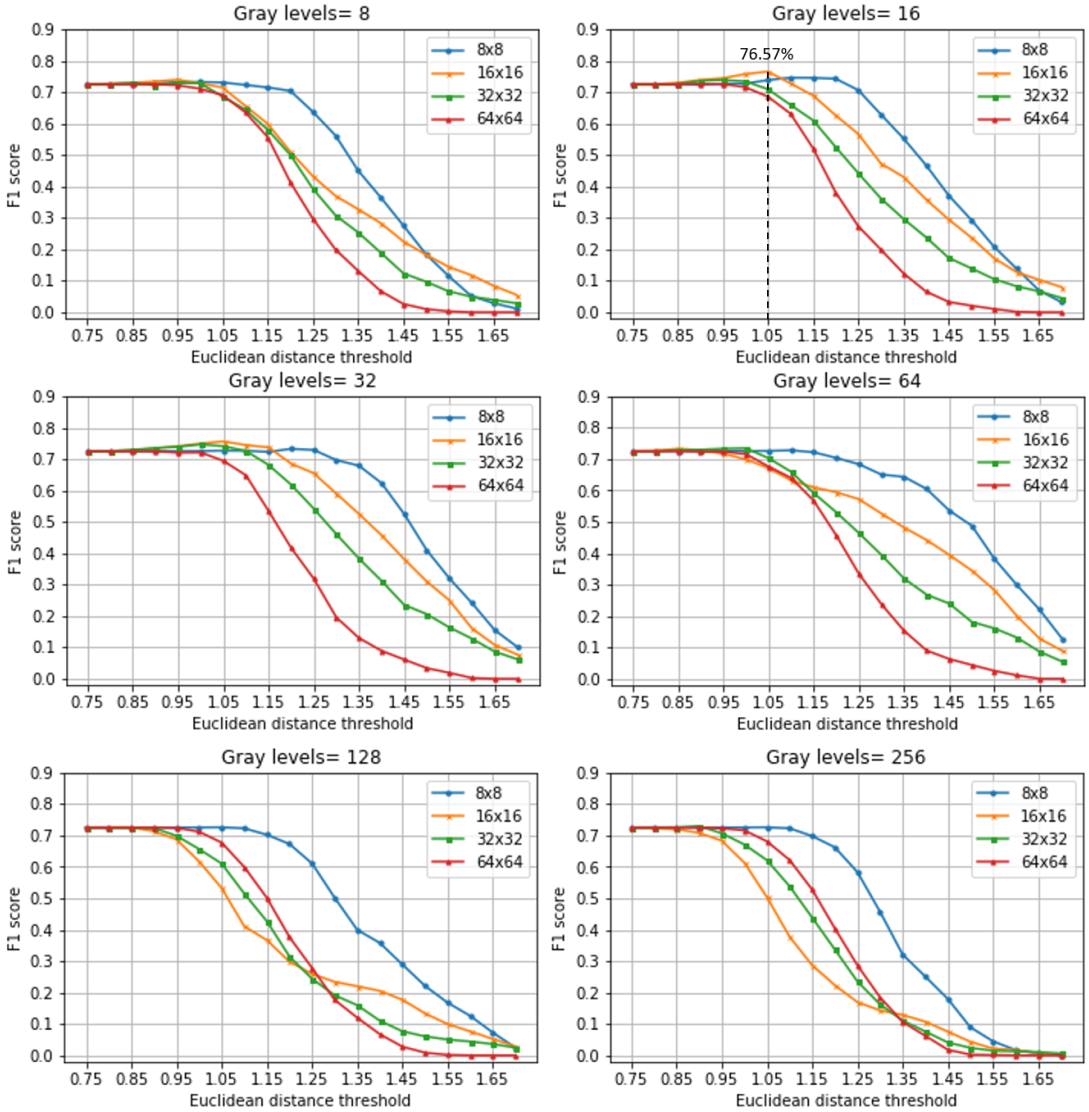

Figure 5.1: F1 scores for the unsupervised detection with GLCM textural features

The maximum F1 scores for all gray levels and all window sizes lie between 70% and 77%. It can be seen that the global maximum (76.57%) occurs at 16 gray levels, while using a window size of 16x16 at a Euclidean distance threshold of 1.05. In order to investigate which defects were poorly detected in order to result in this relatively low F1 score, the F1 scores per defect at the global maximum were graphed, as shown in Figure 5.2.

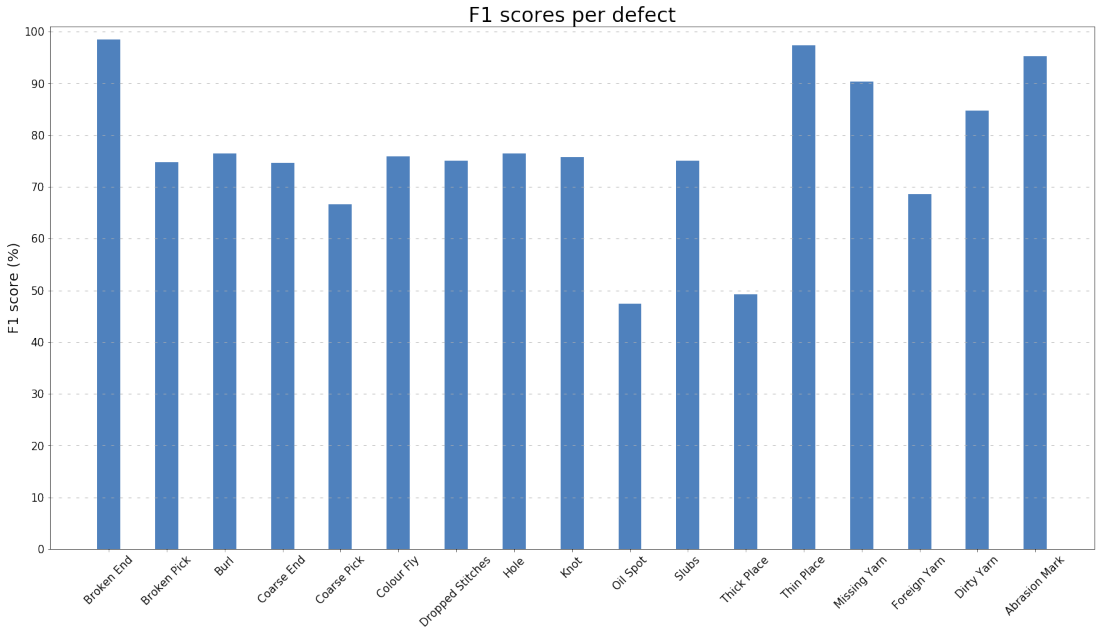

Figure 5.2: F1 scores per defect for the unsupervised detection with GLCM textural features

The two defects with the lowest F1 scores (below 50%) are the oil spot and the thick place. The poor detection is most likely because they were the only two global defects in the dataset As the majority of the image area in the images with these defects were defective, the usage of the same image as the reference has resulted in the reference texture vector characterizing a defective image, rather than a defect-free image. The mediocre F1 score for visually prominent defects that span a fairly large area of the image, such as the hole might also be because of the same reason. This reasoning is further verified as two of the defects with F1 scores over 90%, broken end and abrasion mark, are highly localized and occupy a smaller region of the image they occur in. Therefore, it can be concluded that using the same image as a reference is not practical for global defects.

To remedy the poor detection results from the unsupervised detection approach, a fixed defect-free reference image was used in the next experiment for a supervised detection. The results of the experimented are presented in Figure 5.3.

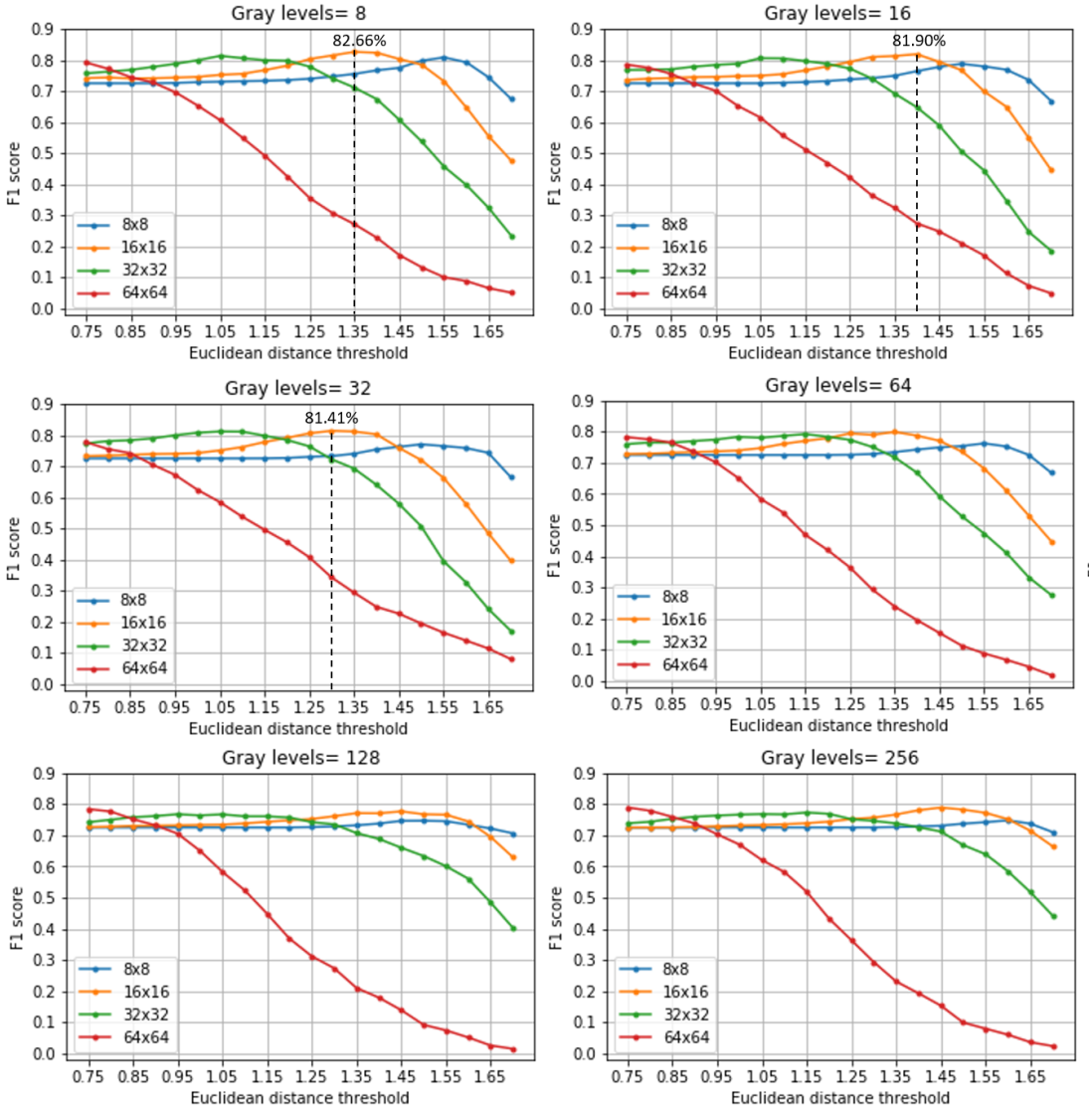

Figure 5.3: F1 scores for the supervised detection with GLCM textural features

A noticeable increase in performance can be seen now that the maximum F1 scores are closer to or above 80% for all gray levels and windows sizes. The maximum F1 scores for the first three gray levels are indicated by dashed lines in Figure 5.3. The global maximum occurs at 8 gray levels, while using a window size of 16x16 at a Euclidean distance threshold of 1.35.

From the graphs presented in Figure 5.3, it can be seen that, in most cases, the F1 score slightly decreases or remains constant when the number of gray levels is

increased for a fixed window size. This result agrees with that of a study [105] in which the classification performance of GLCM features were measured across the full range of quantized grey levels for multiple datasets. In the aforementioned study, it was concluded that the classification performance either stays constant or decreases when gray levels are added. Even though the datasets used in said study comprised of only irregular textures, it can be observed that the same trend applies for regular textures too, judging by the results presented here. However, it can be observed that, when the Euclidean distance threshold is larger (approximately greater than 1.35), the classification F1 scores of 8x8, 16x16 and 32x32 window sizes have increased with increasing gray levels. Since the F1 scores for larger Euclidean distance thresholds are lower than those for smaller thresholds, this trend is not significant in selecting the optimal number of gray levels. However, since this deviates from the expected result, it bears explanation.

A larger Euclidean distance threshold implies that a large difference in the texture vectors of the reference image and each query image is required in order for the query image to be classified as defective. When the number of gray levels are fewer, it is unlikely that such large differences would occur because the range of gray levels is very limited. This, most likely, causes a majority of the images to be classified as defect-free (negative). The spike in false negatives and the drop in true positives causes an overall decrement in recall and precision resulting in a lower F1 score. On the other hand, when the gray levels are larger in number, the range of gray levels and their variance in image subregions are higher. So, the classifier will not have a tendency to label the majority of images as defect-free (negative) like before. Therefore, the recall and precision will not drop as much, even though they will be much lower than those for images with fewer gray levels. However, as mentioned before, this behavior of the graphs at larger Euclidean distance thresholds is not important in the selection of optimal parameters since the F1 scores at these thresholds are much lower than those at smaller Euclidean distance thresholds.

It is noteworthy that a study [122] has claimed that using more gray levels than the range of gray levels in the image would yield poor classification accuracy. Even though the experiment conducted in our research does not explicitly test a range of gray levels greater than the range of gray levels in the image (i.e. 256 gray levels), it can be inferred from the graphs in Figure 5.3 that increasing the number of gray levels further will not bring about an increase in the F1 score because the F1 score steadily decreases when the number of gray levels are increased when the Euclidean distance thresholds are kept fairly small.

Since the maximum F1 score was obtained when using a 16x16 window, it implies that a 16x16 window is small enough to capture the smaller defects in the dataset while being large enough to characterize the texture in the region enclosed by it. The same window size was also chosen as the optimal size by [105] and [109] as well. The former study had arrived at the choice after an extensive analysis of the classification accuracy with varying gray levels and window sizes.

In order to evaluate the detection on each category of defect, the F1 scores per defect at the optimal values were graphed. The grouped bar graph below (Figure 5.4) shows the F1 scores per defect for both the unsupervised and supervised approach and serves as a comparison of the two.

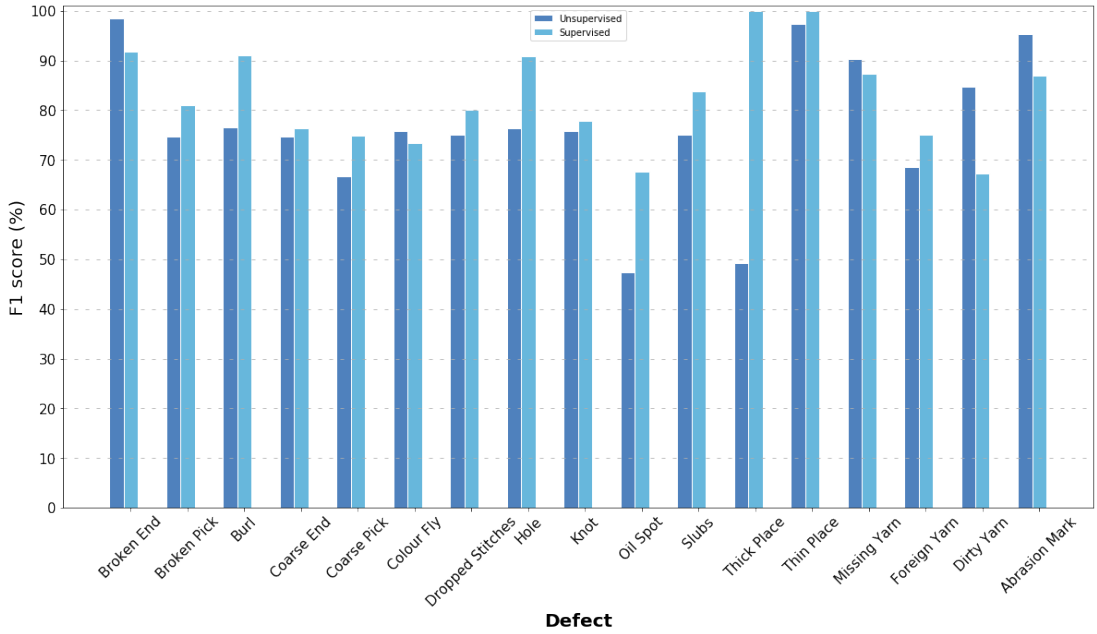

Figure 5.4: F1 scores per defect for detection with GLCM textural features (unsupervised and supervised)

The F1 scores for the global defects, oil spot and thick place, show a significant increase. All defects, except for five, show better results in the supervised approach. As the supervised approach performs well (with F1 scores above 65% for all defects) for the majority of defects and because the unsupervised approach performs poorly for global defects, the supervised approach for feature extraction was selected. In the supervised approach, for all gray levels, a window size of 16x16 provided the maximum F1 score and therefore, it was chosen as the window size for the feature extraction. The number of gray levels was selected as 8 because it provided the best overall F1 score.

The complete list of selected parameters for the GLCM, decided based on experimentation and past research, is given in Table 5.1.

Table 5.1: Selected parameters for the GLCM

Parameter	Selected value
Features	CON, ENE, HOM, COR, ENT
Offset distance (D)	1
Look direction (θ)	0°,45°,90°,135°(averaged)
Window size	16*16
Number of gray levels	8

5.2.2 Results of spectral feature optimization

During the previous experiment, it was decided that a supervised approach involving a defect-free reference image is needed to improve classifier performance. This was mainly because of the presence of global defects in the dataset. Figure 5.5 shows the results of the experimented conducted to determine the vanishing moments and the decomposition level of the discrete wavelet transform. The average F1 score across all defects for each wavelet and each level of decomposition is graphed.

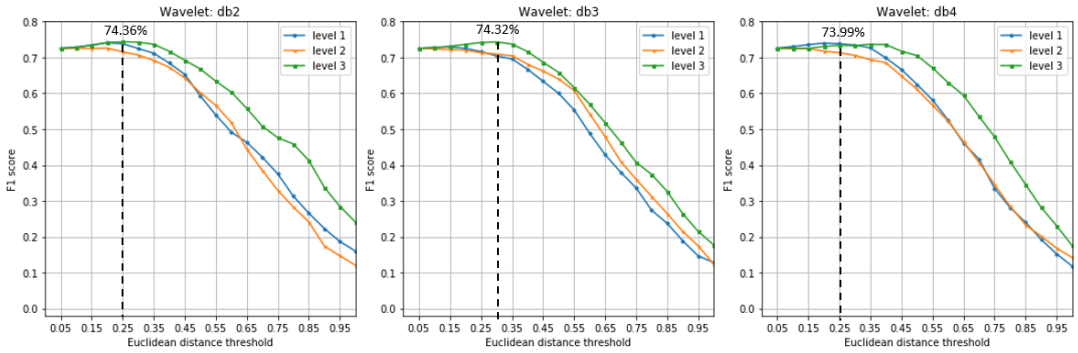

Figure 5.5: F1 scores for the supervised detection with wavelet features)

The maximum F1 score for each wavelet has been indicated in the graphs. Judging by the maximum F1 score, no noticeable change in performance can be seen from these curves. Therefore, the F1 score for each wavelet and each decomposition level were graphed per defect in order to gain more insight into the results. Figure 5.6., Figure 5.7. and Figure 5.8. show the F1 scores per defect

for *db*2, *db*3 and *db*4 respectively, with each cluster of bars representing a defect and each bar representing a level of decomposition. The lighter the colour of the bar, the higher the level of decomposition.

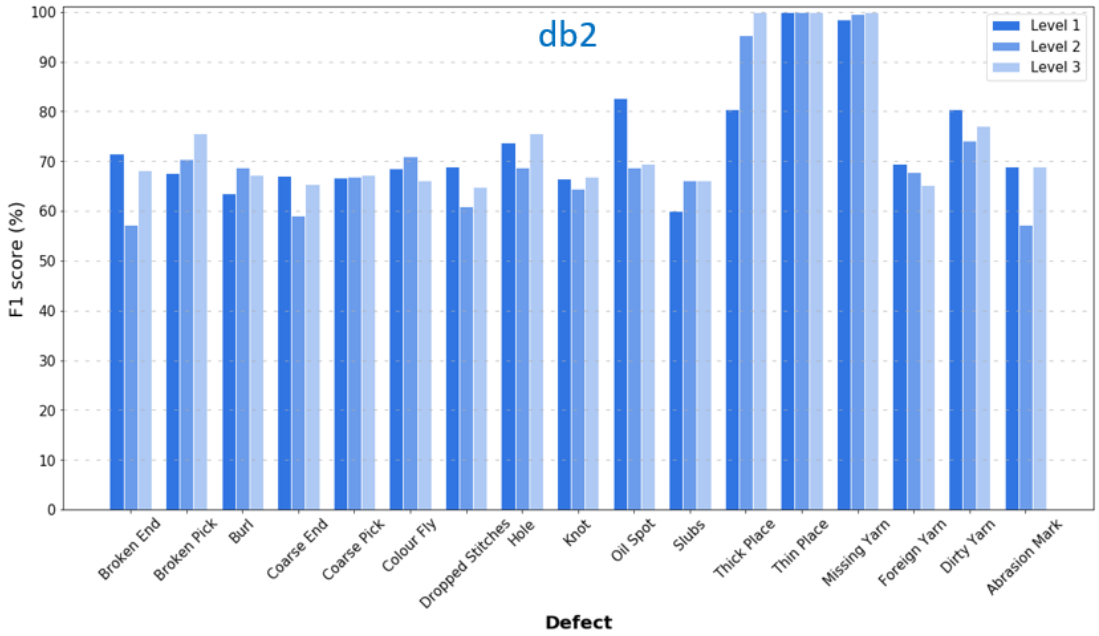

Figure 5.6: F1 scores per defect for detection with the db2 wavelet)

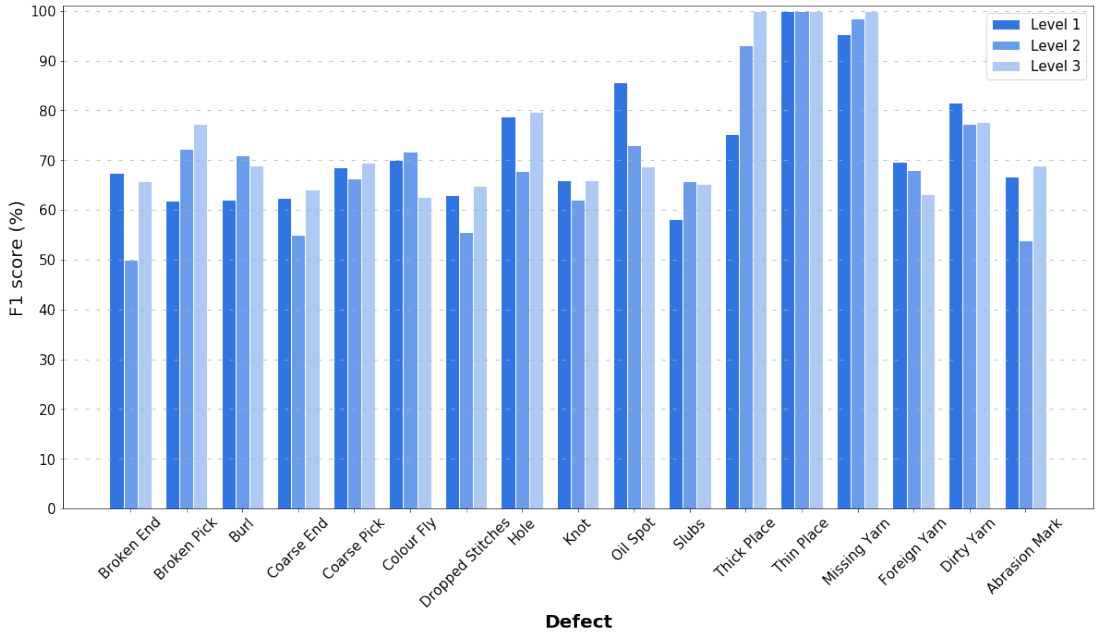

Figure 5.7: F1 scores per defect for detection with the db3 wavelet)

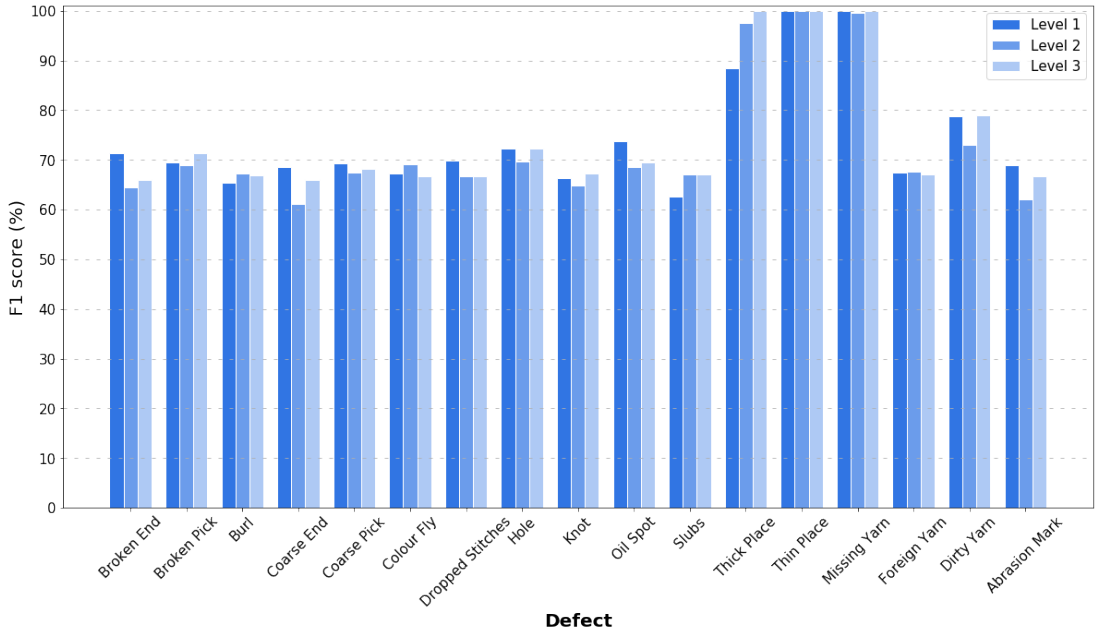

Figure 5.8: F1 scores per defect for detection with the db4 wavelet)

Upon examination of the results, it can be noted that the F1 scores for some defects are higher in some levels than others, regardless of the wavelet used. For example, broken ends are best detected at the first level of decomposition, broken picks are best detected at the third level of decomposition and burls show the highest F1 score in the second level of decomposition. Some defects show comparable F1 scores in multiple levels e.g. knots (levels 1 and 3), slubs (levels 2 and 3) while the thin place is detected almost perfectly at all levels. This implies that different defects in the dataset respond to different scalings of the wavelet. This implication is apparent by the images of defects shown in Table 3.1. It is clear that different types of defects distort the fabric yarn structure to different degrees e.g. a hole is basically a puncture in the fabric and so the yarn structure is absent at a hole whereas laddering or thick place causes the yarns to be pulled apart and a thin place causes the yarn to bunch up together. This results in different edge frequencies at the defect, thereby responding to wavelets with frequencies similar to respective edge frequencies.

Owing to this analysis, it has been concluded that there is no single level of

decomposition that would suit all defects. Therefore, features at all levels will be extracted. The decision of using features at all three levels have also been chosen in [56] and [92] resulting in fairly high classification accuracies.

Among the three wavelets, *db*3 gives the maximum F1 scores for all defects except for broken ends, coarse ends, dropped stitches and knots. Even though they are not maximal, F1 scores between 60% and 70% are shown even for the four aforementioned defects. Therefore, it has been concluded that the *db*3 wavelet, which has 3 vanishing moments should be used to carry out the discrete wavelet transformation.

The complete list of selected parameters for the discrete wavelet transform is given in Table 5.2

Table 5.2: Selected parameters for the discrete wavelet transform

Parameter	Selected value
Mother wavelet	Daubechies *db*
Number of vanishing moments (D)	3 (*db*3)
Type of decomposition	Mallat decomposition
Number of decomposition levels	1, 2 and 3

5.2.3 Results of feature ranking

The fifteen features in the feature set were ranked to obtain the results tabulated in Table 5.3

It can be observed that the textural features and the local entropy are ranked higher than the spectral features. This implies that defective and defect-free images are more distinguishable from each other by the differences in texture and local entropy rather than the spectral information contained in them. This result does not agree with the findings in [53] in which the classifier performance when using textural features only were shown to be similar to that when using spectral features only. It should be noted, however, that the aforementioned

Table 5.3: Results of the feature ranking using Joint Mutual Information (JMI)

Feature	JMI score	Rank
HOM	0.207	1
ENT	0.193	2
LE_STD	0.180	3
ENE	0.173	4
COR	0.113	5
CON	0.049	6
H3	0.037	7
V1	0.028	8
V2	0.020	9
H1	0.019	10
D1	0.014	11
D3	0.014	12
D2	0.010	13
V3	0.010	14
H2	0.004	15

study had not succeeded in detecting four types of defects from the categories of defects they were considering and the two preprocessing steps used in our research before extracting the GLCM were not implemented in said study. The lack of the preprocessing, i.e. gray-level re-quantization and image tiling, has most likely led to the poorer performance of their classifier when using textural features only.

Attempts to remove features of lower ranks from the feature set resulted in a decrease in recall (i.e. more defective images were misclassified) while picking only the top few features resulted in a decrement in all performance metrics. This variation of the performance metrics is shown in Table 5.4 for a k-NN classifier. Hence, it is clear that all fifteen features contribute to improving classifier performance and therefore the full feature set is used for detection in the next section.

5.2.4 Results of defect detection

Five classifiers that are most commonly used in the field of fabric defect detection are compared in Table 5.5. It can be seen that the k-NN classifier clearly

Table 5.4: k-NN classification performance when features are removed from the bottom of the stack and when only the top features are used in the classification

	All 15 features	Top 14 features	Top 13 features	Top 5 features	Top 4 features
Precision	91.97%	93.17%	93.31%	84.81%	82.56%
Recall	96.31%	95.08%	94.46%	85.86%	80.53%
F1 score	93.31%	94.11%	93.89%	85.33%	81.53%
Accuracy	4 94.09%	93.42%	93.19%	83.67%	79.81%

achieves superior classification performance, despite the Naïve Bayes classifier's greater true negative count and smaller false positive count. Therefore, the k-NN classifier is chosen as the binary classifier in this research. The optimal parameter for k used for the k-NN was determined by the combination of a grid search and a 5-fold cross-validation as shown in Figure 5.9. The curves represent the average accuracy and average F1 score for each 5-fold cross-validation and the shaded regions around the validation curves represent the standard deviations of the accuracies and the F1 scores. According to the figure, a k of 5 was chosen as it gave the best classification accuracy and F1 score, whereas the distance was calculated using the Manhattan distance formula.

Table 5.5: Performance of different classifiers on the dataset

Classifier	TP	TN	FP	FN	Precision (%)	Recall (%)	Accuracy (%)	F1 Score (%)
k-NN	470	353	41	18	91.97	96.31	93.31	94.09
Random forest	458	346	48	30	90.51	93.85	91.15	92.15
MLP	425	334	60	63	87.62	87.09	86.05	87.35
SVM	403	339	55	85	87.99	82.58	84.12	85.20
Naive Bayes	274	368	26	214	91.33	56.14	72.78	69.54

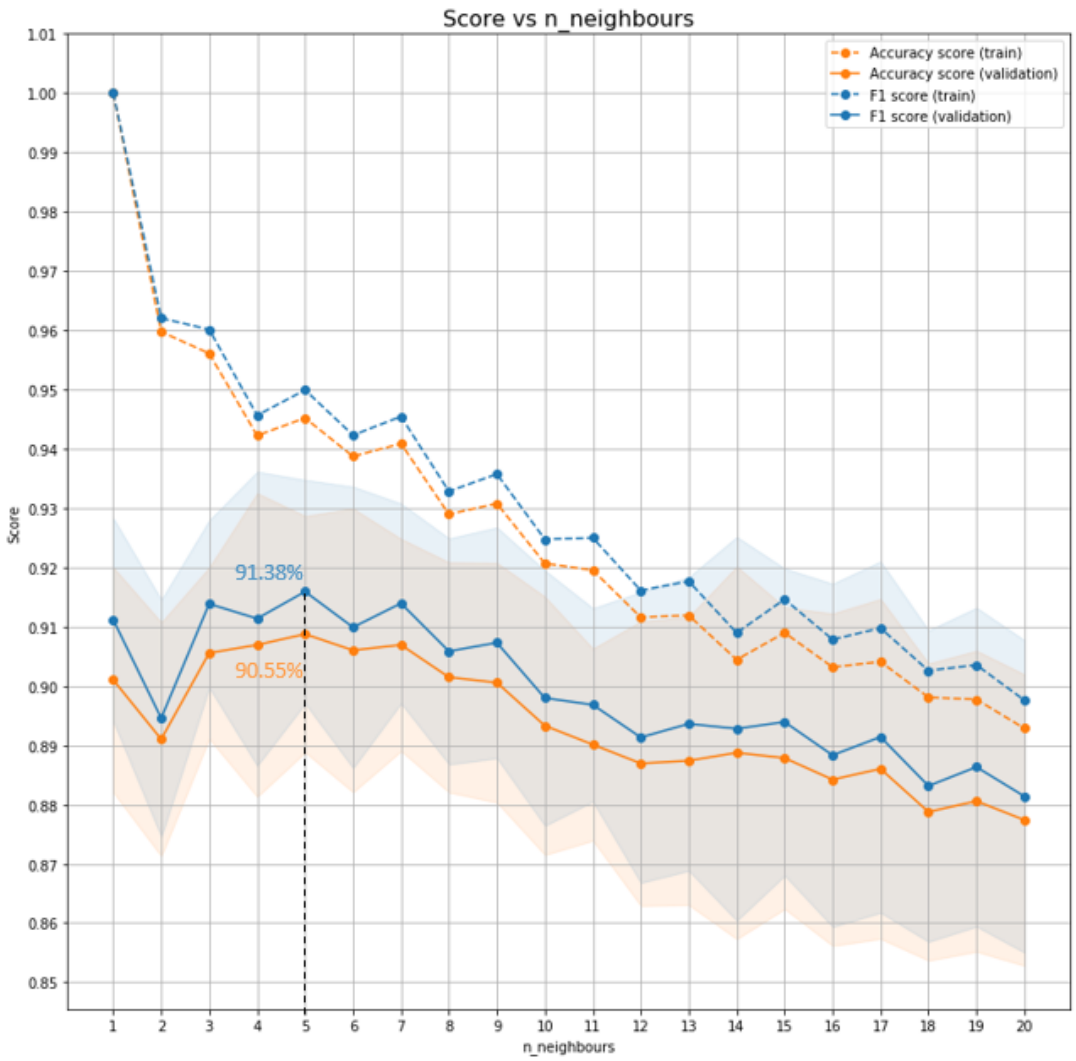

Figure 5.9: Average F1 score and average accuracy vs. number of neighbours (k) for the k-NN 5-fold cross-validation with the Manhattan distance as the distance metric. The shading around the validation line plots show ± 1 standard deviation of the accuracy (in orange) and the F1 score (in blue).

The precision, recall, accuracy and F1 score of the k-NN classifier on each defect type is shown in Table 5.6. It shows that a perfect classification F1 score is obtained for seven types of defects, namely, broken end, dropped stitches, oil spot, thick place, thin place, missing yarn and abrasion mark. It can also be seen that the broken picks, burls, color flies, holes, knots, foreign yarn and dirty yarn

have been classified with F1 scores exceeding 95%. With reference to the feature vector used in the classification, this implies that a combination of the texture distortion, edge variation and gray-level intensity distribution in the locality of these defects is sufficient in distinguishing them from the defect-free areas of the fabric.

The defects that have been classified with comparatively lower accuracies are coarse end, coarse pick and slub. Visual observation of these defects, samples of which are presented in Table 3.1, show that they are quite difficult to distinguish in the image if a defect-free image is not given for reference. The reason for these defects to be misclassified (hence the lower recall) may be a result of their small size. Since these defects only alter the properties of a very limited area around them, the sizes of the windows and structuring element used may not capture these alterations. It may be argued that using smaller windows and a smaller structuring element might help detect these defects. However, the adverse effects of a smaller size, especially the increase in sensitivity to noise, might have a negative effect on the detection of other defects.

5.3 Performance Comparison

In this section, the performance of the proposed method is compared with similar methods. It is to be noted that a majority of the studies on fabric defects have been conducted on one type of fabric — either woven fabrics only [123] [87] or knitted fabrics only [124] [125]. Detection accuracies up to 99% have been obtained in some research [87] [125]. Studies similar to this one, which attempt to develop an algorithm common to both knit and woven fabrics, are fewer in number. One such study [1] has only considered five defects and their classification has achieved an accuracy of 80% for one type defect, while the overall accuracy of classification is approximately 60%. Another study [91] has limited their classification to four defects only, achieving an accuracy of 94%. The

Table 5.6: Performance of the k-NN classifier per defect

Defect type	Precision (%)	Recall (%)	Accuracy (%)	F1 Score (%)
Abrasion Mark	100.00	100.00	100.00	100.00
Broken End	100.00	100.00	100.00	100.00
Broken Pick	100.00	95.24	97.62	97.56
Burl	96.77	96.77	96.77	96.77
Coarse End	77.78	93.33	83.33	84.85
Coarse Pick	93.33	77.78	86.11	84.85
Colour Fly	94.12	100.00	96.88	96.97
Dirty yarn	100.00	96.00	98.00	97.96
Dropped Stitches	100.00	100.00	100.00	100.00
Foreign Yarn	95.24	100.00	97.50	97.56
Hole	93.94	100.00	96.77	96.88
Knot	97.56	93.02	95.35	95.24
Missing yarn	100.00	100.00	100.00	100.00
Oil Spot	100.00	100.00	100.00	100.00
Slub	77.98	97.70	85.06	86.73
Thick Place	100.00	100.00	100.00	100.00
Thin Place	100.00	100.00	100.00	100.00

latter has the highest accuracy achieved in a study of both knitted and woven fabrics, while the former has the most number of defects. It should be noted that studies conducted on detecting more than five defects have only been conducted on either knitted or woven fabrics, but not for both.

In this research, an accuracy of 93.31% has been achieved for a total of 17 defects occurring in both knitted and woven fabrics. So, this study may be considered an extension of [1], with an accuracy almost as high as the accuracy obtained by [91].

5.4 Summary

In this section, the experimental results presented previously are discussed. A comparison of the performance of our method with similar methods used in past work has also been included. In the next section, conclusions are drawn from this

section and the previous ones, the contributions of this work are clearly stated and suggestions for future work are given.

Section 6

Conclusions and Future Work

This section presents the conclusions of this research and summarizes its contributions. Suggestions for continuing this study and improving on the algorithm's performance are also indicated.

6.1 Conclusions

In this paper, a novel combination of features has been used to detect defects in both knitted and woven fabrics. The combined feature set consists of co-occurrence features, wavelet features and a local entropy feature. Classification using a k-NN classifier has yielded an overall accuracy of 93.31%, which is similar to the highest accuracy achieved in similar studies but for a greater number of defects (seventeen defects). Perfect classification accuracies were obtained for seven defect types (broken end, dropped stitches, oil spot, thick place, thin place, missing yarn and abrasion mark) whereas very high accuracies were obtained for seven other defect types (broken picks, burls, color flies, holes, knots, foreign yarn and dirty yarn). Three defects (coarse end, coarse pick, slub) showed lower classification accuracies.

6.2 Contributions

The combination of features used for detection in this study are unique and has proven to provide high classification accuracies across a wide range of defects,

provided they are unprinted and unpatterned. The proposed approach has also performed well for both knit and woven fabrics.

Section 5.3. details the contribution of this research in expanding the number of defect types that can be detected with automatic inspection. The accuracy of detection achieved in this study, i.e. 93.31%, has been shown to be very close to the accuracy of the existing state-of-the-art — 94% [91].

Additionally, an extended dataset has been created for the purpose of this research by modifying the public dataset available from Cotton Incorporated. The dataset comprises 3084 images of 46 types of unprinted and unpatterned knit and woven fabrics.

6.3 Future Work

The dataset used in this study comprises images captured under stable lighting conditions. However, the illumination on the factory floor of a garment manufacturing plant may fluctuate due to ambient light changes and uneven spatial distribution of the lighting system. Future work can focus on appropriate preprocessing steps to mitigate the adverse effects of such conditions.

Feature extraction with the GLCM is a computationally-expensive task that hinders our approach from being implemented real-time. Ways in which the GLCM can be optimized for real-time operation must be explored prior to installation in the production floor.

References

[1] C. S. Cho, B. M. Chung, and M. J. Park, "Development of real-time vision-based fabric inspection system," *IEEE Transactions on Industrial Electronics*, vol. 52, no. 4, pp. 1073–1079, 2005.

[2] R. Fu, M. Shi, H. Wei, and H. Chen, "Fabric defect detection based on adaptive local binary patterns," in *2009 IEEE International Conference on Robotics and Biomimetics (ROBIO)*, 2009, pp. 1–12.

[3] D. M. Tsai and C. Y. Heish, "Automated surface inspection for directional textures," *Image and Vision Computing*, vol. 18, no. 1, pp. 49–62, 1999.

[4] S. Guan and X. Shi, "Fabric defect detection based on wavelet decomposition with one resolution level," in *2008 International Symposium on Information Science and Engineering*, Shanghai, 2008, pp. 281–285.

[5] A. Islam, S. Akhter, and T. E. Mursalin, "Automated textile defect recognition system using computer vision and artificial neural networks," *International Journal of Materials and Textile Engineering*, vol. 2, no. 1, pp. 110–115, 2008.

[6] P. M. Shanbhag, M. P. Deshmukh, and S. S. R, "Overview: Methods of automatic fabric defect detection," *Global Journal of Engineering Design and Technology*, vol. 1, no. 2, pp. 42–46, 2012.

[7] R. S. Sabennian and M. E. Paramasivam, "Defect detection and identification in textile fabrics using multi resolution combined statistical and spatial frequency method," in *2nd International Advance Computing Conference (IACC)*, Patiala, India, 2010, pp. 162–166.

[8] S. Kelegama, J. Wijayasiri, T. Fonseka, D. Fonseka, R. Epaarachchi, F. Foley, S. Wickramasinghe, and D. Weerakon, *Ready-made Garment Industry in Sri Lanka: Facing the Global Challenge*, 1st ed. Institute of Policy Studies Sri Lanka, 2004.

[9] H. A. Abou-Taleb and A. T. M. Sallam, "On-line fabric defect detection and full control in a circular knitting machine," *Autex Research Journal*, vol. 8, no. 1, pp. 21–29, 2008.

[10] R. J. Kadkol, H. M. Rai, and A. H. Kulkarni, "Textile defect detection for fabric material using texture feature extraction," *International Journal of Latest Trends in Engineering and Technology*, vol. 2, no. 2, pp. 173–176, 2013.

[11] S. Guan, X. Shi, H. Cui, and Y. Song, "Fabric defect detection based on wavelet characteristics," in *IEEE Pacific-Asia Workshop on Computational Intelligence and Industrial Application*, 2008, pp. 366–370.

[12] A. Patel, *Towards Zero Defects: Plug Profit Leak*, 1st ed. Meena Publishers, 1974.

[13] M. R. U. Repon and M. A. Al-Mamun, "Study on various faults, their causes and possible remedies of knitting and finishing sections of composite knit industries," *OmniScience: A Multi-disciplinary Journal*, vol. 3, no. 1, pp. 16–25, 2013.

[14] A. Kumar, "Computer-vision-based fabric defect detection: A survey," *IEEE Transactions on Industrial Electronics*, vol. 55, no. 1, pp. 348–363, 2008.

[15] R. G. Saeidi, M. Latifi, S. S. Najar, and A. G. Saeidi, "Computer vision-aided fabric inspection system for on-circular knitting machine," *Textile Research Journal*, vol. 75, no. 6, pp. 492–497, 2005.

[16] M. Patil, S. Verma, and J. Wakode, "A review on fabric defect detection techniques," *International Research Journal of Engineering and Technology (IRJET)*, vol. 4, no. 9, pp. 131–136, 2017.

[17] G. Nikam, L. Meena, A. Shrivastava, and P. Sankadiya, "Fabric defect detection and identification: A survey," *International Journal of Advance Research in Science and Engineering*, vol. 6, no. 4, pp. 817–827, 2017.

[18] M. T. Habib, R. H. Faisal, M. Rokonuzzaman, and F. Ahmed, "Automated fabric defect inspection: A survey of classifiers," *International Journal in Foundations of Computer Science and Technology (IJFCST)*, vol. 4, no. 1, pp. 17–25, 2014.

[19] K. Sakhare, A. Kulkarni, M. Kumbhakarn, and N. Kare, "Spectral and spatial domain approach for fabric defect detection and classification," in *2015 International Conference on Industrial Instrumentation and Control (ICIC)*, Pune, India, 2015, pp. 640–644.

[20] S. Convery, T. Lunney, A. Hashim, and M. McGinnity, "Automated fabric inspection," *International Journal of Clothing Science and Technology*, vol. 6, no. 5, pp. 15–19, 1994.

[21] A. Ranasinghe, S. Madurawala, J. Su, and S. C. Thushara, "An empirical investigation of labor shortage in the manufacturing sector in sri lanka," Department of Accounting, Finance and Economics, Griffith University, 2016.

[22] A. Basu, J. K. Chandra, P. K. Banerjee, S. Bhattacharyya, and A. K. Datta, "Sub image based eigen fabrics method using multi-class SVM classifier for the detection and classification of defects in woven fabric," in *2012 Third International Conference on Computing, Communication and Networking Technologies (ICCCNT'12)*, 2012, pp. 1–6.

[23] S. Priya, T. A. Kumar, and V. Paul, "A novel approach to fabric defect detection using digital image processing," in *Proceedings of 2011 Interna-*

tional Conference on Signal Processing, Communication, Computing and Networking Technologies, 2011, pp. 228–232.

[24] P. Sengottuvelan, A. Wahi, and A. Shanmugam, "Automatic fault analysis of textile fabric using imaging systems," *Research Journal of Applied Sciences*, vol. 3, no. 1, pp. 26–31, 2008.

[25] J. Huart and J. G. Postaire, "Integration of computer vision on to weavers for quality control in the textile industry," in *Proceedings of SPIE*, 1994, pp. 155–163.

[26] R. M. Haralick, K. Shanmugam, and I. Dinstein, "Textural features for image classification," *IEEE Transactions on Systems, Man, and Cybernetics*, vol. SMC-3, no. 6, pp. 610–621, 1973.

[27] Norton-Wayne, M. Bradshaw, and A. J. Jewell, "Machine vision inspection of web textile fabric," in *Proceedings of the British Machine Vision Conference*, 1992, pp. 217–226.

[28] R. Stojanovic, P. Mitropulos, C. Koulamas, Y. Karayiannis, S. Koubias, and G. Papadopoulos, "Real-time vision-based system for textile fabric," *Real-Time Imaging*, vol. 7, no. 6, pp. 507–518, 2001.

[29] M. Bradshaw, "The application of machine vision to the automated," *Mechatronics*, vol. 5, no. 2/3, pp. 233–243, 1995.

[30] J. S. Lane, "Textile fabric inspection system," U.S. Patent 5774177, Jun. 1998.

[31] A. Conci and C. B. Proenca, "A computer vision approach for textile," *Textile Research Journal*, vol. 70, no. 4, pp. 347–350, 2000.

[32] I. Tsai, C. Lin, and J. Lin, "Applying an artificial neural network to pattern recognition in fabric defects," *Textile Research Journal*, vol. 65, no. 3, pp. 123–130, 1995.

[33] A. L. Amet, A. Ertüzün, and A. Erçil, "Texture defect detection using subband domain co-occurrence matrices," in *Proceedings of the 1998 IEEE Southwest Symposium on Image Analysis and Interpretation*, 1998, pp. 205–210.

[34] R. N. Rösler, "Defect detection in fabrics by image processing," *Melliand-Text.ber.*, vol. 73, p. E292, 1992.

[35] C. N. Rao, S. S. Sastry, K. Mallika, H. S. Tiong, and K. B. Mahalakshmi, "Co-occurrence matrix and its statistical features as an approach for identification of phase transitions of mesogens," *International Journal of Innovative Research in Science, Engineering and Technology*, vol. 2, no. 9, pp. 4531–4538, 2013.

[36] F. Ade, N. Lins, and M. Unser, "Comparison of various filter sets for defect detection in textiles," in *Proceedings of the 7th International Conference on Pattern Recognition*, 1984, pp. 428–431.

[37] C. Neubauer, "Segmentation of defects in textile fabric," in *Proceedings of the 11th International Conference on Pattern Recognition*, 1992, pp. 688–691.

[38] F. Tajeripour, E. Kabir, and A. Sheikhi, "Fabric defect detection using modified local binary patterns," *EURASIP Journal on Advances in Signal Processing*, no. 783898, pp. 1–12, 2008.

[39] P. Li, X. Lin, J. Jing, and L. Zhang, "Defect detection in fabrics using local binary patterns," *IGTA 2014: Advances in Image and Graphics Technologies*, vol. 437, pp. 274–283, 2014.

[40] H. Sari-Sarraf and J. S. Goddard, "On-line optical measurement and monitoring of yarn density in woven fabrics," in *Proceedings of SPIE*, 1996, pp. 444–452.

[41] D. M. Tsai and T. Y. Huang, "Automated surface inspection for statistical textures," *Image and Vision Computing*, vol. 21, no. 4, pp. 307–323, 2003.

[42] I. S. Tsai and M. C. Hu, "Automatic inspection of fabric defects using an artificial neural network technique," *Textile Research Journal*, vol. 18, no. 1, pp. 474–482, 1996.

[43] J. G. Campbell and F. Murtagh, "Automatic visual inspection of woven textiles using a two-stage defect detector," *Optical Engineering*, vol. 37, no. 9, pp. 2536–2542, 1998.

[44] C. W. Therrien, *Decision, Estimation, and Classification.* Wiley, 1989.

[45] J. G. Campbell, A. A. Hasim, and F. D. Murtagh, "Flaw detection in woven textiles using space-dependent fourier transform," 1997.

[46] A. Kumar and G. Pang, "Defect detection in textured materials using gabor filters," *IEEE Transactions on Industry Applications*, vol. 38, no. 2, pp. 425–440, 2002.

[47] A. Bodnarova, M. Bennamoun, and S. J. Latham, "A constrained minimisation approach to optimise gabor filters for detecting flaws in woven textiles," in *2000 IEEE International Conference on Acoustics, Speech, and Signal Processing. Proceedings*, 2000, pp. 3606–3609.

[48] A. Bodnarova, M. Bennamoun, and S. J. Latham, "Textile flaw detection using optimal gabor filters," in *Proceedings of the 15th International Conference on Pattern Recognition*, 2000, pp. 799–802.

[49] A. Kumar and G. Pang, "Fabric defect segmentation using multi-channel blob detectors," *Optical Engineering*, vol. 39, no. 12, pp. 3176–3190, 2000.

[50] A. Kumar and G. Pang, "Defect detection system for quality assurance using automated visual inspection," U.S. Patent 6753965, Jun. 2004.

[51] H. Y. Jiang, M. Dong, and W. Li, "Detection of fabric defect based on optimal tree structure of wavelet decomposition," in *2009 International Symposium on Intelligent Ubiquitous Computing and Education*, 2009, pp. 210–213.

[52] H. Jiang, M. Dong, and W. Li, "The detection for fabric defect based on two-dimensional orthogonal wavelet," in *2009 International Conference on Machine Learning and Cybernetics*, 2009, pp. 2470–2472.

[53] S. Sadaghiyanfam, "Using gray-level-co-occurrence matrix and wavelet transform for textural fabric defect detection: A comparison study," in *2018 Electric Electronics, Computer Science, Biomedical Engineerings' Meeting (EBBT)*, Istanbul, 2018, pp. 23–27.

[54] V. V. Karlekar, M. S. Biradar, and K. B. Bhangke, "Fabric defect detection using wavelet filter," in *2015 International Conference on Computing Communication Control and Automation*, 2015, pp. 712–715.

[55] T. I. Su, H. W. Chen, G. B. Hong, and C. M. Ma, "Automatic inspection system for defects classification of stretch knitted fabrics," in *Proceedings of the 2010 International Conference on Wavelet Analysis and Pattern Recognition*, 2010, pp. 125–129.

[56] S. G. Liu and P. G. Qu, "Inspection of fabric defects based on wavelet analysis and BP neural network," in *2008 International Conference on Wavelet Analysis and Pattern Recognition*, Hong Kong, 2008, pp. 232–236.

[57] L. Shuguang and Q. Pingge, "Fabric defects' automatic inspection based on computer vision," in *2nd International Congress on Image and Signal Processing*, 2009, pp. 1–5.

[58] Z. Kang, C. Yuan, and Q. Yang, "The fabric defect detection technology based on wavelet transform and neural network convergence," in *Proceeding of the IEEE International Conference on Information and Automation*, 2013, pp. 597–601.

[59] S. Kim, M. H. Lee, and K. B. Woo, "Wavelet analysis to fabric defects detection in weaving processes," in *Proceedings of the IEEE International Symposium on Industrial Electronics*, 1999, pp. 1406–1409.

[60] W. L. S. Jie, "Feature extraction and detection method of fabrics," China Patent 106203536, Aug. 2016.

[61] F. S. Cohen and Z. Fan, "Rotation and scale invariant texture classification," in *Proceedings of the IEEE Conference on Robotics and Automation*, 1988, pp. 1394–1399.

[62] R. Cross and A. K. Jain, "Markov random field texture models," *IEEE Transactions on Pattern Analysis and Machine Intelligence*, vol. PAMI-5, no. 1, pp. 25–39, 1983.

[63] F. S. Cohen, Z. Fan, and S. Attali, "Automated inspection of textile fabrics using textural models," *IEEE Transactions on Pattern Analysis and Machine Intelligence*, vol. 8, no. 13, pp. 803–808, 1991.

[64] S. Ozdemir and A. Ercil, "Markov random fields and karhunen-loòve transforms for defect inspection of textile products," in *Proceedings of the International Conference on Emerging Technologies and Factory Automation (EFTA)*, 1996, pp. 697–703.

[65] G. Yunan, "Study on image analysis for fabric defects," Ph.D. dissertation, China Textile University, Shanghai, China, 1999.

[66] S. F. Attali and F. S. Cohen, "Surface inspection based on stochastic modeling," in *Proceedings of the Society of Photo-Optical Instrumentation Engineers (SPIE)*, 1986, pp. 46–52.

[67] D. P. Brzakovic, P. R. Bakic, N. S. Vuiovic, and H. Sari-Sarraf, "A generalized development environment for inspection of web materials," in *Proceedings of the IEEE Conference on Robotics and Automation*, 1997, pp. 1–8.

[68] D. Brzakovic, N. Vuiovic, and A. Liakopoulos, "An approach to quality control of texture web materials," in *Proceedings of the SPIE*, 1995, pp. 60–69.

[69] P. D. McNicholas, "Model-based clustering," *Journal of Classification*, vol. 33, no. 3, pp. 331–373, 2016.

[70] J. G. Campbell, C. Fraley, F. Murtagh, and A. E. Raftery, "Linear flaw detection in woven textiles using model-based clustering," *Pattern Recognition Letters*, vol. 18, no. 14, pp. 1539–1548, 1997.

[71] K. Y. Kong, J. Kittler, M. Petrou, and I. Ng, "Chromato-structural approach towards surface defect detection in random textured images," in *Proceedings of the SPIE*, 1994, pp. 193–204.

[72] A. Kumar, "Neural network based detection of local textile defects," *Pattern Recognition Letters*, vol. 36, no. 7, pp. 1645–1659, 2003.

[73] A. Kumar, "Automated defect detection in textured materials," Ph.D. dissertation, The University of Hong Kong, Pokfulam, Hong Kong, 2001.

[74] T. Maenpaa, M. Turtinen, and M. Pietikainen, "Real-time surface inspection," *Real-Time Imaging*, vol. 9, no. 5, pp. 289–296, 2003.

[75] C. C. Hung and I. C. Chen, "Neural-fuzzy classification for fabric," *Textile Research Journal*, vol. 71, no. 3, pp. 220–224, 2001.

[76] S. Y. Liu, L. D. Zhang, Q. Wang, and J. J. Liu, "BP neural network in classification of fabric defect based on particle swarm optimization," in *Proceedings of the 2008 International Conference on Wavelet Analysis and Pattern Recognition*, 2008, pp. 30–31.

[77] J. F. Jing, H. Ma, and H. H. Zhang, "Automatic fabric defect detection using a deep convolutional neural network," *Coloration Technology*, vol. 135, no. 3, pp. 213–223, 2019.

[78] S. Mei, Y. Wang, and G. Wen, "Automatic fabric defect detection with a multi-scale convolutional denoising autoencoder network model," *Sensors (Basel)*, vol. 18, no. 4, pp. 1–18, 2018.

[79] L. Weninger, M. Kopaczka, and D. Merhof, "Defect detection in plain weave fabrics by yarn tracking and fully convolutional networks," in *2018 IEEE International Instrumentation and Measurement Technology Conference (I2MTC)*, 2008, pp. 1–6.

[80] Y. Li, W. Zhao, and J. Pan, "Deformable patterned fabric defect detection with fisher criterion-based deep learning," *IEEE Transactions on Automation Science and Engineering*, vol. 14, no. 2, pp. 1256–1264, 2017.

[81] M. Behravan, R. Boostani, F. Tajeripour, and Z. Azimifar, "A hybrid scheme for online detection and classification of textural fabric defects," in *2009 Second International Conference on Machine Vision*, 2009, pp. 118–122.

[82] B. Julesz, "Textons, the elements of texture perception, and their interactions," *Nature*, vol. 290, no. 5802, pp. 91–97, 1981.

[83] T. Leung and J. Malik, "Representing and recognizing the visual appearance of materials using three-dimensional textons," *International Journal of Computer Vision*, vol. 43, no. 1, pp. 29–44, 2001.

[84] M. Li, Z. M. Deng, and L. Wang, "Defect detection of patterned fabric by spectral estimation technique and rough set classifer," in *Conference: 2013 Fourth Global Congress on Intelligent Systems (GCIS)*, 2013, pp. 190–194.

[85] G. Vladimir, I. Evgen, and N. L. Aung, "Automatic detection and classification of weaving fabric defects based on digital image processing," in *2019 IEEE Conference of Russian Young Researchers in Electrical and Electronic Engineering*, 2019, pp. 2218–2221.

[86] M. M. Mottalib, M. T. Habib, M. Rokonuzzaman, and F. Ahmed, "Fabric defect classification with geometric features using Bayesian classifier," in *Proceedings of 2015 3rd International Conference on Advances in Electrical Engineering*, 2015, pp. 137–140.

[87] V. Murino, M. Bicego, and I. A. Rossi, "Statistical classification of raw textile defects," in *2008 15th IEEE International Conference on Image Processing*, Cambridge, UK, 2004, pp. 311–314.

[88] V. T. Hoang and A. Rebhi, "On comparing color spaces for fabric defect classification based on local binary patterns," in *2018 IEEE 3rd International Conference on Signal and Image Processing*, 2018, pp. 297–300.

[89] L. Yueyang, J. Gaoming, C. Honglian, X. Febglin, and L. Haichi, "Fabric defect detection method based on single-classification support vector machine (SVM)," China Patent 106204543, Dec. 2016.

[90] W. Li, S. Jie, and M. Xue, "Feature extraction and detection method for fabric defects," China Patent 106203536B, May. 2019.

[91] R. Karayiannis, Stojanovic, P. Mitropoulos, C. Koulamas, T. Stouraitis, T. Koubias, and G. Papadopoulos, "Defect detection and classification on web textile fabric using multiresolution decomposition and neural networks," in *ICECS'99. Proceedings of ICECS '99. 6th IEEE International Conference on Electronics, Circuits and Systems (Cat. No.99EX357)*, Paphos, Cyprus, 1999, pp. 765–768.

[92] J. Liu and B. Zuo, "The recognition of fabric defects using wavelet texture analysis and LVQ neural network," in *2009 2nd International Congress on Image and Signal Processing*, Tianjin, 2009, pp. 62–66.

[93] B. Venkatesan, U. S. Ragupathy, P. Vidhyalakshmi, and B. Vinoth, "Inspection of faults in textile web materials using wavelets and ANFIS," in *2012 International Conference on Machine Vision and Image Processing (MVIP)*, 2012, pp. 189–192.

[94] X. Yang, G. Pang, and N. Yung, "Fabric defect classification using wavelet frames and minimum classification error training," in *Conference Record of the 2002 IEEE Industry Applications Conference. 37th IAS Annual Meeting (Cat. No.02CH37344)*, 2002, pp. 290–296.

[95] X. Yang, G. Pang, and N. Yung, "Robust fabric defect detection and classification using multiple adaptive wavelets," in *IEE Proceedings - Vision, Image and Signal Processing*, 2005, pp. 715–723.

[96] C. Incorporated, "Standard fabric defect glossary," https://www.cottoninc.com/quality- products/textile-resources/fabric-defect-glossary, accessed: 2019-01-30.

[97] S. Jayade, D. T. Ingole, and M. D. Ingole, "Skin cancer detection using gray level co-occurrence matrix feature processing," in *2020 5th International Conference on Devices, Circuits and Systems (ICDCS)*, 2020, pp. 49–53.

[98] P. Katiyar and K. Singh, "A comparative study of lung cancer detection and classification approaches in CT images," in *2020 7th International Conference on Signal Processing and Integrated Networks (SPIN)*, 2020, pp. 135–142.

[99] D. A. Gustian, N. L. Rohmah, G. F. Shidik, A. Z. Fanani, and R. A. Pramunendar, "Classification of troso fabric using SVM-RBF multi-class method with GLCM and PCA feature extraction," in *2019 International Seminar on Application for Technology of Information and Communication (iSemantic)*, 2019, pp. 7–11.

[100] A. A. Hamdi, M. S. Sayed, M. M. Fouad, and M. M. Hadhoud, "Fully automated approach for patterned fabric defect detection," in *2016 Fourth International Japan-Egypt Conference on Electronics, Communications and Computers (JEC-ECC)*, 2016, pp. 48–51.

[101] C. H. Chan and G. K. H. Pang, "Fabric defect detection by fourier analysis," *IEEE Transactions on Industry Applications*, vol. 36, no. 5, pp. 1267–1276, 2000.

[102] J. Mohamed and S. Faouzi, "Fabric defect detection using image analysis," in *International Conference of Applied Research in Textile*, 2013, pp. 1–3.

[103] S. Guan, "Fabric defect detection based on fusion technology of multiple algorithm," in *2010 2nd International Conference on Signal Processing Systems*, Dalian, 2010, pp. 553–557.

[104] P. Gong, J. D. Marceau, and P. J. Howarth, "A comparison of spatial feature extraction algorithms for land-use classification with SPOT HRV data," *Remote Sensing of Environment*, vol. 40, pp. 137–151, 1992.

[105] D. Clausi, "An analysis of co-occurrence texture statistics as a function of grey level quantization," *Canadian Journal of Remote Sensing*, vol. 28, no. 1, pp. 45–62, 2002.

[106] A. Baraldi and F. Parmiggiani, "An investigation of the textural characteristics associated with gray level cooccurrence matrix statistical parameters," *IEEE Transactions on Geoscience and Remote Sensing*, vol. 33, no. 2, pp. 293–304, 1995.

[107] M. Umaselvi, S. S. Kumar, and M. Athithya, "Color based urban and agricultural land classification by GLCM texture features," in *IET Chennai 3rd International on Sustainable Energy and Intelligent Systems (SEISCON 2012)*, Tiruchengode, 2012, pp. 49–52.

[108] A. Bodnarova, J. A. Williams, M. Bennamoun, and K. K. Kubik, "Optimal textural features for flaw detection in textile materials," in *TENCON '97 Brisbane - Australia. Proceedings of IEEE TENCON '97. IEEE Region 10 Annual Conference. Speech and Image Technologies for Computing and Telecommunications (Cat. No.97CH36162)*, Brisbane, 1997, pp. 307–310.

[109] S. A. Cuenca and A. Camara, "New texture descriptor for high-speed web inspection applications," in *Proceedings of the 2003 International Conference on Image Processing*, Barcelona, 2003, pp. 537–540.

[110] M. Unser, "Texture classification and segmentation using wavelet frames," *IEEE Transactions on Image Processing*, vol. 4, no. 11, pp. 1549–1560, 1995.

[111] S. Borah, E. L. Hines, and M. Bhuyan, "Wavelet transform based image texture analysis for size estimation applied to the sorting of tea granules," *Journal of Food Engineering*, vol. 79, no. 2, pp. 629–639, 2007.

[112] S. Livens, P. Scheunders, V. D. Wouwer, and D. V. Dyck, "Wavelets for texture analysis, an overview," in *Sixth International Conference on Image Processing and Its Applications*, Antwerp, 1997, pp. 581–585.

[113] W. K. Wong, C. W. M. Yuen, D. D. Fan, L. K. Chan, and E. H. K. Fung, "Stitching defect detection and classification using wavelet transform and BP neural network," *Expert Systems with Applications*, vol. 36, no. 2, pp. 3845–3856, 2009.

[114] Y. Li and X. Di, "Fabric defect detection using wavelet decomposition," in *2013 3rd International Conference on Consumer Electronics, Communications and Networks*, Xianning, 2013, pp. 308–311.

[115] V. V. Karlekar and M. S. Biradar, "Genetic algorithm based wavelet filter for automatic fabric defect detection," in *2015 International Conference on Computer, Communication and Control (IC4)*, Indore, 2015, pp. 54–59.

[116] S. Guan, J. Yuan, and K. Ma, "Fabric defect detection based on wavelet reconstruction," in *International Conference on Multimedia Technology*, Hangzhou, 2011, pp. 3520–3523.

[117] S. Liu and P. Qu, "Fabric defects' automatic inspection based on computer vision," in *2009 2nd International Congress on Image and Signal Processing*, Tianjin, 2009, pp. 139–143.

[118] H. Y. T. Ngan, G. K. H. Pang, S. P. Yung, and M. K. Ng, "Defect detection on patterned jacquard fabric," in *32nd Applied Imagery Pattern Recognition Workshop, 2003. Proceedings*, Washington DC, 2003.

[119] H. H. Yang and J. Moody, "Data visualization and feature selection: New algorithms for nongaussian data," in *Advances in Neural Information Processing Systems*, 2000, pp. 687–693.

[120] J. Suto, S. Oniga, and P. P. Sitar, "Comparison of wrapper and filter feature selection algorithms on human activity recognition," in *2016 6th International Conference on Computers Communications and Control (ICCCC)*, 2016, pp. 124–129.

[121] G. Brown, A. Pocock, M. J. Zhao, and M. Luján, "Conditional likelihood maximisation: A unifying framework for information theoretic feature selection," *Journal of Machine Learning Research*, vol. 13, pp. 27–66, 2012.

[122] M. B. Patel, J. J. Rodriguez, and A. F. Gmitro, "Effect of gray-level requantization on co-occurrence based texture analysis," in *2008 15th IEEE International Conference on Image Processing*, San Diego, 2008, pp. 585–588.

[123] A. S. Malek, "Online fabric inspection by image processing technology," Ph.D. dissertation, Dept. Mech. Eng., University of Upper Alsace, Mulhouse, France, 2012.

[124] K. Hanbay, M. F. Talu, O. F. Özgüven, and D. Öztürk, "Real-time detection of knitting fabric defects using shearlet transform," *Tekstil ve Konfeksiyon*, vol. 29, no. 1, pp. 1–10, 2019.

[125] Z. Musa, T. A. A. Kadir, and R. A. Bakar, "Textile web defect inspection by feature analysis method," in *Second International Conference on Innovative Computing, Information and Control (ICICIC 2007)*, Kumamoto, Japan, 2007, pp. 376–379.